UNIVERSIDAD DE CHILE
FACULTAD DE CIENCIAS FÍSICAS Y MATEMÁTICAS
DEPARTAMENTO DE INGENIERÍA INDUSTRIAL

CONSTRAINING EVAPORATING PRIMORDIAL BLACK HOLES WITH PLANCK DATA

MEMORIA PARA OPTAR AL TÍTULO DE
INGENIERO CIVIL INDUSTRIAL

JUAN PABLO BRANDT URENDA

PROFESOR GUÍA:
DOMENICO SAPONE

MIEMBROS DE LA COMISIÓN:
BLAS DUARTE ALLEUY
FELIPE VILDOSO CASTILLO

Este trabajo ha sido parcialmente financiado por FONDECYT Regular N. 1200171

SANTIAGO DE CHILE
2024

RESUMEN DE LA MEMORIA PARA OPTAR
AL TÍTULO DE INGENIERO CIVIL INDUSTRIAL
POR: JUAN PABLO BRANDT URENDA
FECHA: 2024
PROF. GUÍA: DOMENICO SAPONE

RESTRINGIENDO AGUJEROS NEGROS PRIMORDIALES CON LOS DATOS DE PLANCK

En un Universo en expansión, la cosmología física emerge como la clave para desvelar los misterios acerca de la naturaleza a gran escala del Universo. Dos de estos misterios son la naturaleza de la materia oscura, que corresponde al 26 % de la composición del Universo, y la discrepancia entre las estimaciones de la tasa actual de expansión del Universo por las mediciones de la radiación de fondo de microondas y la escalera de distancia local, llamada tensión de Hubble. Por lo tanto, este trabajo busca continuar el trabajo de Nesseris et al. (2020) restringiendo, con los datos del telescopio espacial *Planck*, el modelo de agujeros negros primordiales, que supone que una fracción de la materia oscura consiste en agujeros negros primordiales (esto es, regiones muy densas y pequeñas que colapsan) para entender mejor la naturaleza de la materia oscura y reducir la tensión de la constante de Hubble. Para esto, se utilizan simulaciones de cadenas de Markov como método de inferencia estadística para estimar los parámetros cosmológicos, junto con las funciones de verosimilitud del fondo cósmico de microondas del telescopio *Planck*.

Los agujeros negros primordiales (PBHs por sus siglas en inglés) ya han sido considerados para proveer la materia oscura. Sin embargo, ningún trabajo anterior utiliza todos los datos del telescopio *Planck* y sus funciones de verosimilitud asociadas para restringir PBHs que se evaporan modelados como un fluido acoplado con radiación. En este trabajo, se estiman los parámetros cosmológicos para el modelo PBH, encontrando parámetros de mejor ajuste estadísticamente consistentes con el modelo ΛCDM para pequeñas fracciones de PBHs explicando la materia oscura, pero que aumentan el parámetro de Hubble a $72.9 \pm 1.0\,\mathrm{km\,s^{-1}\,Mpc^{-1}}$ para una fracción mayor a 0.1.

Este trabajo está limitado por la dependencia del parámetro de Hubble en las ecuaciones dinámicas de PBH, lo que sesga el modelo imponiendo que Hubble sea exactamente el mismo de ΛCDM. Otra limitación es suponer que todos los PBHs tienen la misma masa inicial, lo que no es completamente cierto, y no considerar la teoría de perturbaciones, sino sólo el fondo. Queda propuesto usar funciones extendidas de masa para PBHs y tomar en cuenta la teoría de perturbaciones, junto con modificar el código `CLASS` para evitar la dependencia mencionada en la ecuaciones para PBH y radiación oscura.

Abstract

In an expanding Universe, physical cosmology emerges as the key to unveiling the mysteries surrounding the large-scale nature of the Universe. Two of these mysteries are the nature of dark matter, which corresponds to 26 % of the composition of the Universe, and the discrepancy between today's estimations of the expanding rate of the Universe by the cosmic microwave background and the local distance ladder measurements, called Hubble tension. Therefore, this work aims to continue the work of Nesseris et al. (2020) by constraining with *Planck* data the primordial black hole model, which assumes that a fraction of dark matter consists of primordial black holes (that is, overdense and very small regions that collapse), to understand better the nature of dark matter and reduce the Hubble tension. For this, Markov chain simulation is used as an statistical inference method to estimate the cosmological parameters, along with the *Planck* cosmic microwave background likelihood functions.

Primordial black holes (PBHs) have been considered before as providing dark matter. However, none uses all the *Planck* data and its associated likelihood functions to constrain evaporating PBHs modeled as a coupled fluid with radiation. In this work, the cosmological parameters are estimated for the PBH model, finding best fits statistically consistent with the ΛCDM model for small fractions of PBHs explaining dark matter, but that raise the Hubble parameter to $72.9 \pm 1.0\,\mathrm{km\,s^{-1}\,Mpc^{-1}}$ for a fraction higher than 0.1.

This work is limited by the dependence of the Hubble parameter on the PBH dynamical equations, which biases the model on imposing Hubble to be exactly the same as the ΛCDM one. Another limitation is assuming that all PBHs have the same initial mass, which is not completely true, and not considering perturbation theory, but only the background. It is proposed using extended mass functions for PBHs and taking perturbation theory into account, along with modifying the `CLASS` code to avoid the mentioned dependence on PBH and dark radiation equations.

AMDG

Acknowledgments

I want to thank God first, who inspired me every time before starting to work on this project, and St. Thomas Aquinas, whose prayer helped me get assistance from above to understand clearly and develop the complex concepts of cosmology. I also thank my family, especially my parents and Teresa, who supported me and put up with me during my long studies at Universidad de Chile.

I thank Domenico, my advisor, whose knowledge and recommendations served as a guide for developing this work properly, and Blas, my co-advisor, whose feedback was always very valuable to be able to bring cosmology to the world of engineering. Thanks also to Daniela and Bayron for helping me answer my questions.

Finally, I thank everyone who has contributed to this work coming to fruition, whether by praying or talking with me about the subject.

This research used resources of the National Energy Research Scientific Computing Center (NERSC), a U.S. Department of Energy Office of Science User Facility located at Lawrence Berkeley National Laboratory, operated under Contract No. DE-AC02-05CH11231 using NERSC's JupyterHub.

Table of Content

List of Tables

List of Figures

Chapter 1

Introduction

1.1 General background

In a dynamical Universe, physical cosmology emerges as the key to unveiling the mysteries surrounding the large-scale nature of the Universe. One of these mysteries is the nature of dark matter, which explains some physical phenomena, such as the behavior of the galactic rotation curves and corresponds to 26 % of the composition of the Universe, while all the known matter (called baryonic matter for its components) represents only 5 % and the remaining 69 % accounts for dark energy (Planck Collaboration, Aghanim, N., et al., 2020b). Another mystery is the Hubble tension, namely the discrepancy between today's estimations of the expanding rate of the Universe by the cosmic microwave background and the local distance ladder measurements (Hu & Wang, 2023). Therefore, this work aims to continue the work of Nesseris et al. (2020) by constraining with *Planck* data the primordial black hole model, which assumes that a fraction of dark matter consists of primordial black holes (that is, overdense and very small regions that collapse), to understand better the nature of dark matter and reduce the Hubble tension.

Considering the subject at hand, it is convenient to previously define the concept of physical cosmology. According to Peebles (1993), physical cosmology is the study of "the large-scale nature of the material world around us, by the methods of the natural sciences" (p. 3), that is the study of the origin, development and end of the Universe as a whole (Ryden, 2006). Various models have been proposed, called cosmologies or cosmological models, to explain the behavior of the Universe. In particular, the standard cosmological model or ΛCDM presents an expanding Universe composed principally of baryonic matter, radiation and cold dark matter (CDM)[1], characterized by a positive cosmological constant Λ. This model has several cosmological parameters, like the Hubble constant H_0, which represents the expanding rate of the Universe today; the radiation density $\Omega_{r,0}$; the total matter density $\Omega_{m,0}$, which characterize the amount of non-relativistic matter of the Universe (composed of CDM, baryons and, possibly, heavy neutrinos); the dark energy density $\Omega_{\Lambda,0}$; the equation of state of dark energy parameter w_Λ, which characterize how dark energy behaves; and

[1]It is known as "cold" dark matter because the particles that compose it have non-relativistic velocities, that is, very much lower than the speed of light in vacuum.

the matter density perturbation amplitude $\sigma_{8,0}$, which is the root-mean-square error of the matter density fluctuations at scales of 8 Mpc (Weinberg, 2008)[2]. According to this model, as already mentioned, it is estimated that 69 % of the composition of the Universe corresponds to dark energy (DE), 26 % to dark matter (DM) and only 5 % to baryonic matter (Planck Collaboration, Aghanim, N., et al., 2020b). Despite constituting much of the Universe, what dark energy and matter are, is still unknown. However, its existence is accepted, since it is believed to be necessary for explaining certain physical phenomena, like the accelerated expansion of the Universe (Perlmutter et al., 1999; Riess et al., 1998) and the galactic rotation curves' behavior (Rubin & Ford, 1970).

Before describing primordial black holes, the proper subject of this work, it is necessary to define what black holes and gravitational waves are. Black holes, predicted by Schwarzschild (1916) based on Einstein's 1915 general theory of relativity and observed for the first time in 2017 (The Event Horizon Telescope Collaboration et al., 2019), are generated by the gravitational collapse of very massive stars and consist of spacetime regions with a very intense gravitational field, such that not even light can escape or avoid falling into them (Wald, 1984). Less than 60 years after its proposal, Hawking (1974, 1975) discovered that black holes are thermodynamic objects, because they have a non-zero temperature, emit radiation and, thus, lose mass. In particular, primordial black holes (PBHs), proposed by Zel'dovich and Novikov (1967), are believed to have been formed from the collapse of large overdensities after the Big Bang in the radiation dominated era (Carr & Hawking, 1974; Hawking, 1971), so they are not made up of baryonic matter (because they formed before the epoch in which matter and radiation existed in equal measure). On the other hand, gravitational waves (GWs) are generated by very massive accelerated objects and consist of small perturbations that propagate through spacetime (Misner et al., 1973). They were predicted by Einstein (1915) and detected for the first time a hundred years after, when its emission was observed from the merger of two black holes (Abbott et al., 2016).

The nature of dark matter is still unknown. However, since their prediction by the general relativity theory and recent measurements provided by the detection of gravitational waves, it has become reasonable to substitute dark matter particles with overdense and very small regions that collapse (primordial black holes). In fact, the consideration of evaporating PBHs as dark matter could provide the necessary amount of gravity to form the galaxy halos attributed to dark matter. One way to test the PBH model is by looking at its energy injection in the cosmic microwave background (CMB)[3], being discarded if it produces too much radiation. However, if the latter is true, PBHs could still serve to reduce the Hubble tension by raising its parameter.

1.2 Project description

The importance of studying primordial black holes lies in the fact that they provide "a unique probe of four areas of physics: (1) the early Universe ($M < 10^{15}$ g); (2) gravitational collapse ($M > 10^{15}$ g); (3) high energy physics ($M \sim 10^{15}$ g); and (4) quantum gravity

[2]Mpc stands for one million (mega) parsecs, a unit of length used to measure large distances.

[3]The cosmic microwave background is the 300 000 years old Universe.

($M \sim 10^{-5}\,\mathrm{g}$)" (Carr & Kühnel, 2021, p. 7)[4]. As regards (1), considering very light PBHs could help reduce the Hubble tension, but it can not explain the amount of dark matter in the Universe. On the other hand, as regards (2), PBHs with higher mass could explain 26 % of the Universe, which corresponds to dark matter, because they have not been completely evaporated by now.

Dark matter corresponds to 26 % of the Universe's composition and has been studied since its proposition by Zwicky in 1933 until today (Misiaszek & Rossi, 2023). However, and although it is believed that its existence is necessary to explain some phenomena that occur in the Universe, as the galactic rotation curves being flat for large radii[5] (Rubin & Ford, 1970), the gravitational lensing effect[6] in the large scale structure of the Universe (Massey et al., 2007) and the temperature anisotropies of the cosmic microwave background[7] (Planck Collaboration et al., 2016), dark matter's nature is still unknown. There are many candidates for dark matter (Arbey & Mahmoudi, 2021), such as weakly interacting massive particles (WIMPs) (Roszkowski et al., 2018) and axions (Weinberg, 1978), but they have not yet been discovered experimentally. As an alternative, the PBH model assumes that a part of dark matter consists of primordial black holes, given that since they lose mass in the form of radiation, their matter density can couple with radiation as a fluid. Thus, this model can help to understand better what is the nature of dark matter by estimating cosmological parameters.

Several recent works consider the possibility of primordial black holes providing the Universe's dark matter. However, none uses *Planck* data and its associated likelihood to constrain evaporating PBHs modeled as a radiation-coupled fluid. Carr et al. (2016) analyze theoretically the three mass ranges where this is plausible, introducing "a novel scheme for investigating the compatibility of a general extended PBH mass function with arbitrary constraints" (p. 27), extended by Carr and Kühnel in 2020 and 2021, with an emphasis on the intermediate mass range (mentioned in the PBH model section); Nesseris et al. (2020) estimate the cosmological parameters using Markov chain simulation and "found that the PBH model is statistically consistent with ΛCDM according to the AIC statistical tool[8]" (p. 7), which serves as a basis for this work; Escrivà et al. (2022) exhaustively review all the literature about PBHs, focusing "on their formation, their role as dark matter candidates and their manifold signatures" (p. 1), and also mentioning future prospects of observations, allowing the author to delve deeper into PBH theory; and Mazde and Visinelli (2023) "consider a scenario where PBHs incidentally affect the formation of DM by temporarily meddling with the thermal history of the Universe" (p. 2).

Another problem that has been studied for a few years is the Hubble tension, namely the discrepancy between the CMB and the local measurements of the Hubble constant, used to

[4]In this quote, M denotes the mass of the PBHs.

[5]A galactic rotation curve consists of the speed of objects orbiting a galaxy concerning the radial distance from its center. Without dark matter, the galaxy orbiting objects' speed should decrease when increasing distance from its center due to gravity.

[6]The gravitational lensing effect consists of the curvature of spacetime for light's path by a massive body between a distant object and the observer, causing light to bend as if there were a lens.

[7]The cosmic microwave background anisotropies correspond to the fluctuations of the order µK in its temperature.

[8]AIC is the Akaike Information Criterion (Akaike, 1974).

infer the age and fate of the Universe and also the distance to galaxies, among others (Riess & Breuval, 2023). The expansion of the Universe was discovered by Lemaître (1927) and Hubble (1929) independently, based on Slipher's 1915 observations of recession velocities of galaxies. This expansion is given by the Hubble function H and, today, by the Hubble constant H_0, which has been measured using different methods, like the Cepheid-based calibration[9], yielding $H_0 = 73.04 \pm 1.04\,\mathrm{km\,s^{-1}\,Mpc^{-1}}$ (Riess et al., 2022); and CMB radiation's observed temperature and polarization fluctuations, yielding values of $67.4 \pm 0.5\,\mathrm{km\,s^{-1}\,Mpc^{-1}}$ (Planck Collaboration, Aghanim, N., et al., 2020b). This difference between astrophysical and cosmological estimates of the Hubble constant could be reduced by considering primordial black holes that have already evaporated but have released enough radiation to raise H_0.

Some recent works aim to solve the Hubble tension by considering lighter PBHs. Regarding the existence of low mass PBHs, Cheek et al. (2023) suggest "that the production of GWs from the evaporation of PBHs is amongst the most robust signals that could be searched for with observations in the future regarding the existence of light PBHs in the early Universe" (p. 13); Nesseris et al. (2020) consider very light PBHs to raise the CMB induced Hubble constant to $70.5\,\mathrm{km\,s^{-1}\,Mpc^{-1}}$, serving as a basis for this work; and Ding (2023) proposes "that the merger rate of PBH binaries can constrain the PBH mass function ... [and help to] pin down the Hubble parameter" (p. 10), explaining how PBH binaries can be used to measure the Hubble constant.

1.3 Main objective

In consequence, the main objective of this work is to develop a method, based on statistical inference, to estimate the cosmological parameters when it is supposed that a fraction of the Universe's dark matter consists of primordial black holes, seeking to verify if this model fits reality and helps to understand the nature of dark matter and reduce the Hubble tension, continuing the work of Nesseris et al. (2020).

1.4 Specific objectives

To achieve the main objective, the following specific objectives are defined:

1. Study the PBH model.
2. Install and test the Einstein-Boltzmann `CLASS` code (Blas et al., 2011).
3. Adapt the `CLASS` code to the PBH model and compare its background equations computation with the code used by Nesseris et al. (2020).
4. Estimate the cosmological parameters considering the adapted `CLASS` code to the PBH model with statistical inference methods using *Planck* satellite data (Planck Collabora-

[9] A Cepheid is a radial pulsating variable star.

tion, Akrami, Y., et al., 2020) and CMB likelihoods (Planck Collaboration, Aghanim, N., et al., 2020a).

5. Compare the results with the ΛCDM model (Planck Collaboration, Aghanim, N., et al., 2020b) and those obtained by Nesseris et al. (2020).

The difference between this work and the article by Nesseris et al. (2020) is the consideration of *Planck* data and CMB likelihoods, which had not been taken into account previously due to the complexity of doing so (instead, Nesseris et al. (2020) used an approximate method).

1.5 Scope

The scope of this work is limited to the main and specific objectives previously mentioned and the method used to achieve them. Other data sets and likelihood functions to constrain the primordial black hole model, as well as other cosmologies proposed to understand dark matter and reduce the Hubble tension, are outside the analysis of this work. Extended mass functions for PBHs and perturbation theory are also not considered in this project (for simplicity, the author assumes all PBHs to have the same initial mass and considers only the background equations).

Another limitation is using `CLASS` instead of `CAMB` as the code to compute the background equations for the PBH model. Since, in `CLASS`, the dynamical equations for PBH and dark radiation are written in terms of the scale factor (see the physical cosmology section for more details), they depend on the Hubble parameter. This dependency is a problem because Hubble is also expressed in terms of the PBH and its associated dark radiation matter densities, so the author has to impose the Hubble parameter to be the same as the ΛCDM one, biasing the PBH model.

1.6 Methodology

It is important to define a methodology according to the objectives of this work. As it is part of data science area, an adaptation of CRoss Industry Standard Process for Data Mining (CRISP-DM) methodology will be used throughout it. The adapted CRISP-DM methodology has six phases:

1. Context understanding: Review of recent literature about primordial black holes when considered accounting for a fraction of the Universe's dark matter and to reduce the Hubble tension, and theoretical study of the PBH model itself. In this step, it is expected to achieve the first specific objective.

2. Data understanding: First, download and install *Planck* data and `CLASS` code. Then, test the `CLASS` code by computing background equations and plotting matter, radiation,

and dark energy densities. In this phase, it is expected to reach the second specific objective.

The data are obtained from the 2018 *Planck* release and consist of CMB temperature fluctuation maps (for a detailed description, see the CMB maps section). On the other hand, `CLASS` is a code written in C (with a wrapper to work with Python) designed to compute CMB among other cosmological observables (see the `CLASS` code section for more details).

3. Code adaptation: First, adapt the `CLASS` code to the PBH model by modifying both Python and C files (which make up the code). Second, test the adapted code by computing the background equations and plotting matter, radiation, and dark energy densities. And third, compare the results with those of the code used by Nesseris et al. (2020). In this phase, it is expected to achieve the third specific objective.

4. Modeling: Estimate the cosmological parameters considering the adapted `CLASS` code to the PBH model using Markov chain Monte Carlo methods to evaluate the parameter's likelihood function. First, with a maximum limit of samples[10] and then without constraining its number, using in both cases the *Planck* data and CMB likelihoods.

   For this, the `Cobaya` package (Torrado & Lewis, 2019; Torrado & Lewis, 2021) is used, which contains the `CLASS` code and the *Planck* CMB likelihood functions and allows estimating the parameters employing Markov chain Monte Carlo methods. In this step, it is expected to achieve the fourth specific objective.

5. Evaluation: Compare the results obtained with the values of the cosmological parameters estimated considering the ΛCDM model and those of the article by Nesseris et al. (2020). In this step, it is expected to reach the fifth specific objective.

6. Deployment: Publication of this work.

The adapted CRISP-DM methodology is preferred over others, such as SEMMA (Sampling, Exploring, Modifying, Modeling, and Assessing), since it better adapts to the proposed objectives, specifically for the first phase: a sampling step (as in SEMMA) is not necessary, since the intention is to use all the data, but it is essential to understand the model well before working with the data.

1.7 Outline

The outline of this project is the following. In Chapter 2, the basics of the background universe cosmology is presented. The primordial black hole model and the adaptation of Einstein-Boltzmann `CLASS` code to this model are explained in detail, and sections on statistical inference in cosmology and Markov chain Monte Carlo methods are also included.

In Chapter 3, the data and its associated likelihood functions used throughout this work are detailed.

[10]Here, *samples* mean accepted steps made by the random walkers.

In Chapter 4, the author presents its results, testing the `CLASS` code in the background and estimating the cosmological parameters with Markov chain Monte Carlo methods, first for ΛCDM only and then for the PBH model, considering a limited and unlimited number of samples.

In Chapter 5, a general discussion of the author's results is presented, commenting on the difficulties using the `CAMB` code, the test of the `CLASS` code, and the cosmological parameters estimation for the limited and unlimited cases, analyzing the best fits with its associated errors and the chains convergence, and comparing it with *Planck* and Nesseris et al. (2020) results.

Finally, in Chapter 6, the author concludes with the results obtained in this work, proposing recommendations for future work.

Chapter 2

Conceptual framework

2.1 Physical cosmology

Physical cosmology consists of studying the Universe's nature and behavior at large scales, using natural sciences methods and assuming as a hypothesis the cosmological principle, namely that the Universe's distribution of matter and energy is homogeneous and isotropic at large scales: neither the observer's location nor the direction of sight affect the observational evidence (Peebles, 1993). This assumption is straightforward in a static Universe, but since Lemaître (1927) and Hubble (1929) independently discovered its expansion, the cosmological principle breaks down at lower scales. That is why the large-scale Universe is called the background.

The dynamic of the background is described by the Friedmann equations, derived from the Einstein equations

$$G_{\mu\nu} = \frac{8\pi G}{c^4} T_{\mu\nu}, \tag{2.1}$$

where G is the universal gravitational constant, c is the speed of light in vacuum, $G_{\mu\nu}$ is the Einstein tensor representing the spacetime geometry and $T_{\mu\nu}$ is the energy-momentum tensor, which accounts for Universe's matter and, for a perfect fluid of energy density ρ and pressure p is written as

$$T^{\mu}_{\nu} = (\rho + p) u^{\mu} u_{\nu} + p \delta^{\mu}_{\nu}, \tag{2.2}$$

where u^{μ} is the four-velocity of the fluid considering a comoving frame[11] and δ^{μ}_{ν} is the Kronecker delta, with ρ and p depending on the cosmic time t.

The expansion of the Universe can be parametrized by the Robertson-Walker scale factor a, relating comoving and physical coordinates[12], assuming that it only depends on the cosmic time t to ensure the Universe's homogeneity. Then, the rate of expansion of the Universe can be defined as

$$H(t) \equiv \frac{1}{a} \frac{da}{dt}, \tag{2.3}$$

[11] In a comoving frame, the observer moves with the expansion of the Universe as if inside of it.
[12] In a physical frame, the Universe is observed from outside.

known as the Hubble function, where $H_0 \equiv H(t = t_{\text{today}})$ is the Universe's expansion rate measured today, called the Hubble constant.

From the above, the Friedmann equations can be deduced by taking the time component and the trace of Einstein's equations

$$H^2 = \frac{8\pi G}{3}\rho - \frac{Kc^2}{a^2}, \tag{2.4a}$$

$$3H^2 + \frac{dH}{dt} = -\frac{8\pi G}{c^2}p - \frac{Kc^2}{a^2}, \tag{2.4b}$$

where K represents the curvature of the Universe.

Using equation (2.4), the following conservation law can be found for the matter component

$$\frac{d\rho}{dt} + 3H\left(\rho + \frac{p}{c^2}\right) = 0, \tag{2.5}$$

where if the fluid is adiabatic[13], its pressure can be written as

$$p = w\rho, \tag{2.6}$$

where w is a constant, called the equation of state parameter; and, replacing this in equation (2.5), the following can be found for the fluid's density

$$\rho = \rho_0 \left(\frac{a}{a_0}\right)^{-3(1+w)}, \tag{2.7}$$

where a_0 and ρ_0 are the integration limits (generally, but not always, a_0 and ρ_0 are, respectively, the scale factor and the fluid density measured today).

It is convenient to rewrite equation (2.4a), such that $\Omega + \Omega_K = 1$, defining a normalized density parameter

$$\Omega \equiv \frac{8\pi G}{3H^2}\rho \tag{2.8}$$

and a curvature's normalized density parameter

$$\Omega_K \equiv -\frac{Kc^2}{(aH)^2}, \tag{2.9}$$

where Ω_s represents the normalized density for a specific species s (like matter, radiation, or dark energy, among others) and $\Omega_{s,0} \equiv \Omega_s(t = t_{\text{today}})$ is that density, but measured at present.

Replacing equations (2.7) and (2.8) in (2.4a) the first Friedmann equation can be expressed as

$$H^2 = H_0^2 \sum_s \Omega_{s,0} \left(\frac{a}{a_0}\right)^{-3(1+w_s)}, \tag{2.10}$$

assuming that the Universe is flat ($\Omega_K = 0$) and where 0 stands for the parameters measured today.

[13] A fluid is said to be adiabatic when its pressure only depends on its density.

2.2 The PBH model

Primordial black holes are believed to have been formed, in the radiation era, from the collapse of large overdensities generated during inflation (Carr & Hawking, 1974; Hawking, 1971); and the PBH model proposes considering that a fraction of dark matter could be composed of primordial black holes (Nesseris et al., 2020). It is important to note that these black holes must be primordial to account for dark matter because their formation before the Big Bang nucleosynthesis (BBN) allows the baryon constraint of 5 % to be avoided.

The mass of PBHs, denoted by $M_{\rm PBH}$ is related with its formation time t, following

$$M_{\rm PBH} \sim 10^{15} \left(\frac{t}{10^{-23}\,\mathrm{s}} \right) \mathrm{g}, \tag{2.11}$$

so, according to Carr and Kühnel (2021), "PBHs could span an enormous mass range and are the only ones which could be smaller than a solar mass" (p. 3), but "observations imply that only a tiny fraction of the early Universe could have collapsed into PBHs" (p. 5). However,

> non-evaporating PBHs may still be of great cosmological interest even if they provide only a small fraction of the dark matter. For example, they could play a role in generating the supermassive black holes in galactic nuclei and these provide only 0.1 % of the dark matter. (p. 6)

According to Green and Kavanagh (2021), there is a constrain for the fraction of PBHs: if all dark matter is made up of PBHs, then necessarily $10^{17}\,\mathrm{g} \lesssim M_{\rm PBH} \lesssim 10^{22}\,\mathrm{g}$ (or $10^{23}\,\mathrm{g}$ for others, like Carr et al. (2021)). This is called the asteroidal to sublunar mass region and accounts for the difficulty in finding PBHs. But, according to Carr and Kühnel (2021), the fraction of dark matter in PBHs can be significant also in the intermediate $10^{34}\,\mathrm{g} \lesssim M_{\rm PBH} \lesssim 10^{35}\,\mathrm{g}$ and the extremely large $M_{\rm PBH} > 10^{44}\,\mathrm{g}$ range. On the other hand, PBHs lighter than $5 \times 10^{14}\,\mathrm{g}$ would have evaporated by now, so it can not explain the amount of DM, but it can produce enough radiation to reduce the Hubble tension.

Considering monochromatic mass functions for PBHs[14], if it is assumed that a fraction $f_{\rm PBH}$ of DM consists of PBHs, the PBH matter density can be written as

$$\Omega_{\rm PBH} = f_{\rm PBH} \Omega_c, \tag{2.12}$$

where Ω_c is the cold dark matter density.

At some initial time $a_{\rm in}$, Ω_c can be written in terms of the matter density today, so equation (2.12) remains as

$$\Omega_{\rm PBH} = f_{\rm PBH} \frac{\Omega_{c,0}}{a^3} \frac{M_{\rm PBH}}{M_{\rm in}}, \tag{2.13}$$

where a is the Robertson-Walker scale factor, $\Omega_{c,0}$ is the CDM density measured today and $M_{\rm in}$ is the mass of the black hole population at $a = a_{\rm in}$.

[14] That is, assuming that all PBHs have the same mass.

On the other hand, according to Page (1976), a black hole emits mass as a function of cosmic time t as follows

$$\frac{dM_{\rm BH}}{dt} = -\frac{\alpha\hbar c^4}{G^2}\frac{1}{M_{\rm BH}^2}, \tag{2.14}$$

where $M_{\rm BH}$ is the mass of the black hole (BH), α is a numerical coefficient that depends on $M_{\rm BH}$, $\hbar$ is the reduced Planck's constant, c is the speed of light in vacuum and G is the universal gravitational constant.

Equation (2.14) can be rewritten for PBHs in terms of the scale factor a as

$$\frac{dM_{\rm PBH}}{da} = -\frac{\mathcal{C}}{aH(a)M_{\rm PBH}^2}, \tag{2.15}$$

where $\mathcal{C} \equiv \alpha\hbar c^4/G^2$, H is the Hubble function and $da = aHdt$. This change of variables is necessary because `CLASS` works with the scale factor in the background.

For conservation of energy, if a PBH loses mass, it has to radiate energy, which will be called dark radiation, to avoid confusing it with dark energy. Following the approach of Nesseris et al. (2020), based on Majerotto et al. (2004), matter and dark radiation can be considered to form a coupled fluid, as a consequence of the conservation law expressed in equation (2.5), such that

$$\frac{d\rho_c}{da} + \frac{3}{a}\rho_c = Q(a), \tag{2.16a}$$

$$\frac{d\rho_X}{da} + \frac{3(1+w_X)}{a}\rho_X = -Q(a), \tag{2.16b}$$

where ρ is the density associated with DM (ρ_c) or dark radiation (ρ_X), w_X is the equation of state parameter of dark radiation, $Q(a)$ is a coupling term and the accompanying sign refers to a gain ($-$) or loss ($+$) in energy.

The following dynamic equation for PBHs can be obtained using equations (2.13) and (2.15)

$$\frac{d\Omega_{\rm PBH}}{da} + \frac{3}{a}\Omega_{\rm PBH} = -\frac{\mathcal{C}/M_{\rm in}^3}{a^{10}H}\frac{\left(f_{\rm PBH}\Omega_{c,0}\right)^3}{\Omega_{\rm PBH}^2}, \tag{2.17}$$

where the right side of the equation corresponds to the coupling term $Q(a)$.

Then, according to equation (2.16b), dark radiation follows

$$\frac{d\Omega_X}{da} + \frac{3(1+w_X)}{a}\Omega_X = \frac{\mathcal{C}/M_{\rm in}^3}{a^{10}H}\frac{\left(f_{\rm PBH}\Omega_{c,0}\right)^3}{\Omega_{\rm PBH}^2}. \tag{2.18}$$

It can be seen that the term a^{-10} could generate instabilities at early times, so the system of equations (2.17) and (2.18) can be simplified considering the following normalized energy densities

$$\tilde{\Omega}_{\rm PBH} = a^3\Omega_{\rm PBH}, \tag{2.19a}$$

$$\tilde{\Omega}_X = a^{3(1+w_X)}\Omega_X. \tag{2.19b}$$

Taking equation (2.19) into account, the dynamics of PBH and dark radiation can be written as

$$\frac{d\tilde{\Omega}_{\rm PBH}}{da} = -\frac{\tilde{\alpha}}{aH}\frac{\left(f_{\rm PBH}\Omega_{c,0}\right)^3}{\Omega_{\rm PBH}^2}, \tag{2.20a}$$

$$\frac{d\tilde{\Omega}_X}{da} = \frac{\tilde{\alpha}}{a^{1-3w_x}H}\frac{\left(f_{\rm PBH}\Omega_{c,0}\right)^3}{\Omega_{\rm PBH}^2}, \tag{2.20b}$$

where $\tilde{\alpha} \equiv \mathcal{C}/M_{\rm in}^3$.

Now, it can be asserted that the standard cosmology holds in the early Universe. Thus, at some initial time $a_{\rm in}$, the conditions for PBH and dark radiation will be $\tilde{\Omega}_{\rm PBH}(a_{\rm in}) = f_{\rm PBH}\Omega_{c,0}$ and $\tilde{\Omega}_X(a_{\rm in}) = 0$, respectively. Also, it has to be noticed that there is a problem with the presence of H in (5.1), because it is only defined implicitly; so, it is necessary to assume the Hubble parameter to be the same as the ΛCDM cosmology, considering equation (2.10) as follows

$$H^2 = H_0^2\left[\frac{\Omega_{r,0}}{a^4} + \frac{\Omega_{b,0}}{a^3} + (1-f_{\rm PBH})\frac{\Omega_{c,0}}{a^3} + \Omega_{\rm PBH}(a) + \Omega_X(a) + \Omega_{\Lambda,0}\right], \tag{2.21}$$

with

$$\Omega_{r,0} = \Omega_{\gamma,0}\left[1 + N_{\rm eff}\times\frac{7}{8}\times\left(\frac{4}{11}\right)^{4/3}\right], \tag{2.22a}$$

$$\Omega_{\Lambda,0} = 1 - \Omega_{b,0} - (1-f_{\rm PBH})\Omega_{c,0} - \Omega_{r,0} - \Omega_{\rm PBH}(a=1) - \Omega_X(a=1), \tag{2.22b}$$

where $\Omega_{r,0}$, $\Omega_{b,0}$, $\Omega_{\Lambda,0}$ and $\Omega_{\gamma,0}$ are the radiation, baryonic, dark energy and photon densities today, respectively; and $N_{\rm eff}$ is the total effective number of neutrinos.

2.3 The `CLASS` code

The Cosmic Linear Anisotropy Solving System (`CLASS`) is a cosmology code whose purpose "is to simulate the evolution of linear perturbations in the Universe and to compute CMB and large scale structure observables" (Lesgourgues, 2023). It is written in C and includes a wrapper, written in Cython, to work with Python (Audren, 2014; Blas et al., 2011).

The use of `CLASS` instead of other Boltzmann codes has several advantages, like its user-friendliness (it is easy to understand, compile, and run), flexibility (it can be modified to adapt it to other cosmologies), accuracy (it is accurate at the 0.1 % level) and speed (it is faster than the other Boltzmann codes) (Lesgourgues, 2011). However, it also has an important disadvantage: the background dynamical equations are written with respect to the scale factor instead of the conformal time[15]. This is a problem when considering the PBH model, because the dynamical equations for PBH and its associated dark radiation (when are written in terms of the scale factor) depend on the Hubble parameter, which,

[15]The conformal time $\tau \equiv \int dt/a(t)$ is the time that takes a free particle with velocity c to travel a comoving distance $c\tau$.

in turn, depends on the PBH and dark radiation matter densities (see equations (5.1) and (2.21)). That is why the author has to impose the Hubble parameter to be the same as in ΛCDM, biasing the PBH model. This is not a problem when considering perturbation theory, because its dynamical equations are written in terms of the conformal time; although in this work, for simplicity, only the background equations are considered.

It is convenient to use `CLASS`, which is designed to compute CMB, among other cosmological observables, because the data used in this work consists of CMB maps (see CMB maps section). But, before using `CLASS`, it is necessary to modify the original code by adapting it to the PBH model (described in the PBH model section), being careful of modifying both C and Python files, as `CLASS` is written in this two languages. These changes are described in the `CLASS` code detailed modification appendix.

2.4 Statistical inference in cosmology

In cosmology, the approach to understanding statistics is Bayesian because "data are hard to come by, observations cannot be twisted and repeated ... easily, ... models are characterized by many correlated parameters, and every drop of previous information, even loosely related to a given parameter, has to be taken into account" (Amendola & Tsujikawa, 2010, p. 363). Therefore, probabilities are interpreted "as the degree of belief in a hypothesis" (Verde, 2007, p. 4), based on Bayes and Price's work published after the first's death in 1763. The advantages of this approach for cosmology are "its flexibility in combining results from different observations and in allowing a direct comparison between various parametrizations" (Amendola & Tsujikawa, 2010, p. 356).

With this approach, Bayes' theorem of conditional probabilities allows to estimate the cosmological parameters using statistical inference. This theorem stands that

$$\mathcal{P}(T|D) = \frac{\mathcal{P}(D|T)\mathcal{P}(T)}{\mathcal{P}(D)}, \tag{2.23}$$

where D is the known data x_i, T is the unknown theory or hypothesis (the set of cosmological parameters θ_j specifying a model[16]), the posterior distribution $\mathcal{P}(T|D)$ is the conditional probability of having the theory given the data, the likelihood function $\mathcal{P}(D|T)$ is the conditional probability of having the data given the theory, the prior probability $\mathcal{P}(T)$ is the probability of having the theory and the probability distribution function (PDF) of the data $\mathcal{P}(D)$ is the probability of having the data, also called evidence. Here, the posterior contains the relevant information, that is, "the probability distribution of the parameters given that we observed the data x_i and that we have some prior knowledge about the parameters themselves, ... [based on] the results of previous experiments" (Amendola & Tsujikawa, 2010, p. 358).

Considering this Bayesian approach, the parameter estimation in cosmology works as follows. If there is some known data $\mathbf{x}$, it can be interpreted as a cosmological model (in this case, the PBH model), assumed to be correct and containing the parameters $\boldsymbol{\theta}$ to estimate.

[16] "A model is a theoretical framework ... [assumed to be] true" (Heavens, 2009, p. 2).

"The goal of parameter estimation is to provide estimates of the parameters, and their errors, or ideally the whole probability distribution of $\boldsymbol{\theta}$, given the data $\mathbf{x}$, [that is] ... the posterior probability distribution[17]", $\mathcal{P}(\boldsymbol{\theta}|\mathbf{x})$ (Heavens, 2009, p. 2). From this, the expectation values and the errors[18] of the parameters can be calculated. But often it is not easy to obtain the posterior directly, so here appears Bayes' theorem, which allows calculating the likelihood first (in this case, the *Planck* ones, described in the *Planck* CMB likelihoods section) and then the posterior.

The best-fit parameters for a model can be chosen as those for which the χ^2 parameter is minimum. This statistic is defined by

$$\chi^2 = \sum_{ij} (x_i - \mu_i)\, C_{ij}^{-1}\, (x_j - \mu_j)\,, \tag{2.24}$$

for data x_i, with $\mu_i = \langle x_i \rangle$ the mean of x_i and $C_{ij} = \langle (x_i - \mu_i)\,(x_j - \mu_j) \rangle$ the covariance matrix. If the data are uncorrelated, χ^2 reduces to

$$\chi^2 = \sum_i \frac{(x_i - \mu_i)^2}{\sigma_i^2}, \tag{2.25}$$

with σ_i^2 the data's variance. Then, if χ^2 is minimum, $x_i \approx \mu_i + \sigma_i$ or, in terms of D and T, $D \approx T + \sigma$; thus, by minimizing χ^2, the likelihood is maximized and the best-fit parameters are obtained. Here, the standard deviation σ_i represents the data's error and can be illustrated in contour plots for different confidence intervals as 1σ (or 68 % confidence), 2σ (95 %) or 3σ (99 %).

There are several methods to get the best-fit parameters given a cosmological model by maximizing the likelihood function; one of them is the Markov chain simulation (or Markov chain Monte Carlo), described in the following section.

2.5 MCMC

Markov chain Monte Carlo (or MCMC) is a "general method based on drawing values of [the parameters] $\boldsymbol{\theta}$ from approximate distributions and then correcting those draws to better approximate the target posterior distribution, $\mathcal{P}(\boldsymbol{\theta}|\mathbf{x})$" (Gelman et al., 2021, p. 275). It works sequentially: the sampling distribution depends on the last value drawn, forming a Markov chain[19]. However, the method's success is not given by the Markov property but by the improving distributions at every step in the simulation, looking for convergence, although the Markov property helps to prove this convergence.

When MCMC is applied, various independent sequences $\theta_1, \theta_2, \theta_3, \ldots$ are created, each one "produced by starting at some point θ_0 and then, for each j, drawing θ_j from a transition

[17] The posterior probability distribution "is the probability that the parameter takes certain values, after doing the experiment" (Heavens, 2009, p. 2).

[18] Errors measure the uncertainty in the knowledge of the parameters and can be calculated by taking the standard deviation over the data.

[19] "A Markov chain is a sequence of random variables $\theta_1, \theta_2, \ldots$, for which, for any j, the distribution of θ_j given all previous $\boldsymbol{\theta}$'s depends only on the most recent value, θ_{j-1}" (Gelman et al., 2021, p. 275).

distribution, $T_j(\theta_j|\theta_{j-1})$ that depends on the previous draw, θ_{j-1}" (Gelman et al., 2021, p. 275). This transition distributions are constructed aiming at the convergence of the Markov chain to the posterior distribution, $\mathcal{P}(\boldsymbol{\theta}|\mathbf{x})$.

This method is used when it is difficult (sometimes due to the computer limitation) sampling the parameters directly from the posterior distribution, so MCMC samples in a manner that at every step, it is expected to draw from a distribution approaching the posterior. This is the case in cosmology: due to the large amount of data, it is not possible to sample the cosmological parameters $\boldsymbol{\theta}$ directly from the posterior distribution $\mathcal{P}(\boldsymbol{\theta}|\mathbf{x})$.

One important thing concerning MCMC is getting the chains to converge, making it crucial to consider a test. One of them is the Gelman and Rubin (1992) convergence criterion, defined as

$$R = \frac{\frac{L-1}{L}W + \frac{1}{L}B}{W}, \tag{2.26}$$

where L is the number of remaining values, after discarding D, for each chain,

$$W = \frac{1}{J}\sum_{j=1}^{J} s_j^2, \tag{2.27}$$

with J the number of chains,

$$s_j^2 = \frac{1}{L-1}\sum_{l=1}^{L}\left(x_l^{(j)} - \overline{x}_j\right)^2 \tag{2.28}$$

the within chain variance, with $x_l^{(j)}$ the lth sample from the jth Markov chain,

$$B = \frac{L}{J-1}\sum_{j=1}^{J}\left(\overline{x}_j - \overline{x}_{\cdot}\right)^2 \tag{2.29}$$

the between chain variance,

$$\overline{x}_{\cdot} = \frac{1}{J}\sum_{j=1}^{J}\overline{x}_j \tag{2.30}$$

the grand mean and

$$\overline{x}_j = \frac{1}{L}\sum_{l=1}^{L} x_l^{(j)} \tag{2.31}$$

the chain mean. Here, "under convergence, W and B/L should agree ... [and] R should approach unity as convergence is achieved" (Heavens, 2009, p. 15). Then, if $R_{\min} - 1 \approx 0$, convergence is also achieved and can be an indicator to stop sampling.

Chapter 3

Data description

3.1 CMB maps

The cosmic microwave background, discovered by Penzias and Wilson in 1965, represents the Universe at an age of 300 000 years, making the photons from it the most powerful evidence of the early times, confirming the Big Bang theory and leading to an era of precision cosmology (Dodelson, 2003). From the radiation of the CMB, an average temperature of 2.7 K can be estimated, with fluctuations of the order of µK, called anisotropies, usually plotted as CMB maps.

In this work, data from the 2018 *Planck* satellite release are used, consisting of temperature fluctuation maps of the cosmic microwave background (Planck Collaboration, Akrami, Y., et al., 2020). Specifically, these contain CMB intensity and polarization maps "provided at an approximate angular resolution of 5′ FWHM[20] and HEALPix[21] resolution $N_{\mathrm{side}} = 2048$" (Planck Collaboration, 2020) and produced by four different methods: `Commander`, `NILC`, `SEVEM`, and `SMICA`; which are described below and the corresponding CMB maps are illustrated in Figures 3.1, 3.2, 3.3 and 3.4, respectively.

> `Commander` is a *Planck* software code implementing Bayesian parametric component separation. Each astrophysical signal component is modelled in terms of a small number of free parameters per pixel, typically in terms of an amplitude at a given reference frequency and a small set of spectral parameters, and these are fitted to the data with an MCMC Gibbs sampling algorithm. (Planck Collaboration, 2020)
>
> Needlet Internal Linear Combination (or `NILC` in short) is a blind component separation method for the measurement of Cosmic Microwave Background (CMB) from the multi-frequency observations of sky. It is an implementation of an Internal Linear Combination (ILC) of the frequency channels under consideration with minimum error variance on a frame of spherical wavelets called needlets, allowing localized filtering in both pixel space and harmonic space. (Planck Collaboration, 2020)

[20] This means Full-Width-at-Half-Maximum (FWHM).

[21] The Hierarchical Equal Area isoLatitude Pixelization (HEALPix) "is a versatile structure for the pixelization of data on the sphere" (Górski et al., 2005, p. 1).

SEVEM produces cleaned CMB maps at several frequencies by using a procedure based on template fitting in real space. The templates used in the SEVEM pipeline are typically constructed by subtracting two close *Planck* frequency channel maps, after first smoothing them to a common resolution to ensure that the CMB signal is properly removed. (Planck Collaboration, 2020)

SMICA produces CMB maps by linearly combining *Planck* input channels with multipole-dependent weights, including multipoles up to $\ell = 4000$. Temperature and polarization maps are produced independently. In temperature, two distinct CMB renderings are produced and then merged (hybridized) together into a single CMB intensity map. In polarization, the E and B modes are processed independently and the results are combined to produce Q and U maps[22]. (Planck Collaboration, 2020)

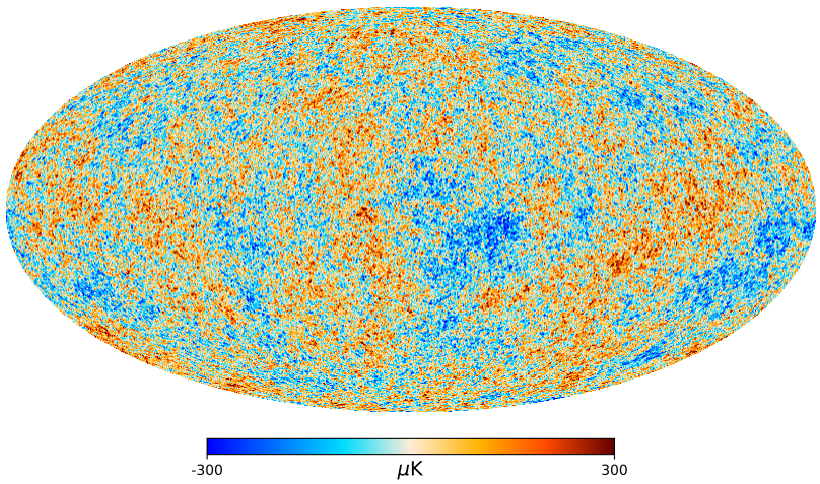

Figure 3.1: Inpainted full-mission CMB map from Commander temperature.

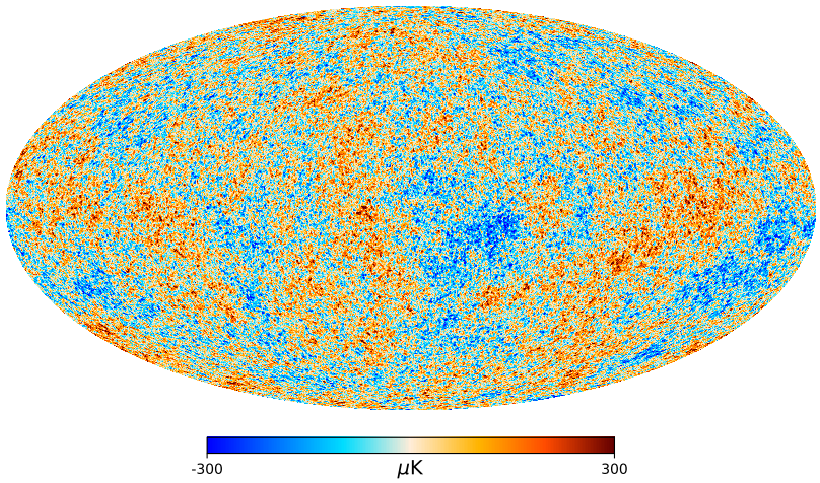

Figure 3.2: Inpainted full-mission CMB map from NILC temperature.

[22]For more details about Q and U polarization, and E and B modes, see the Stokes parameters and polarization appendix.

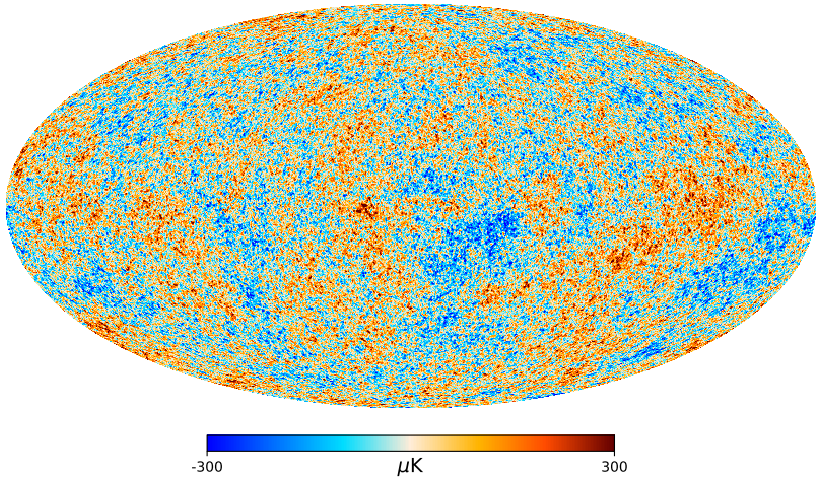

Figure 3.3: Inpainted full-mission CMB map from `SEVEM` temperature.

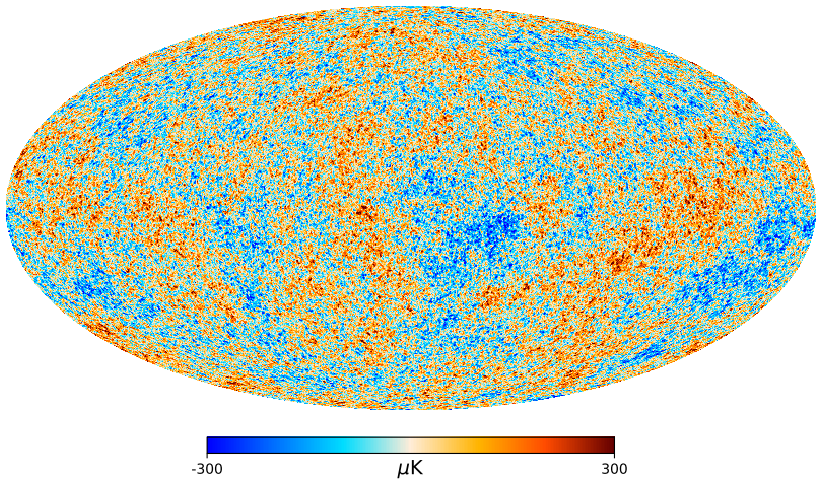

Figure 3.4: Inpainted full-mission CMB map from `SMICA` temperature.

3.2 *Planck* CMB likelihoods

Planck cosmic microwave background likelihoods, derived from the 2018 data release (Planck Collaboration, Aghanim, N., et al., 2020a), are used throughout this work. These "CMB likelihoods are built from estimates of the angular power spectra derived from intensity and linear polarization maps, ... [except for] the LFI[23] 70 GHz low-ℓ polarization likelihood, which is based on maps" (Planck Collaboration, Aghanim, N., et al., 2020a, p. 2). Each likelihood function is described in detail below.

1. Low-ℓ temperature (TT) likelihood: According to Planck Collaboration, Aghanim, N., et al. (2020a) this function "is constructed by approximating the marginal distribution of the temperature angular power spectrum derived from Gibbs sampling-based component separation" (p. 2), based on `Commander`; but it has the disadvantage that is "limited to very low multipoles, typically $\ell \leq 30$" (p. 4). It can be written as

$$\mathcal{L}(C_\ell) \propto \sum_{i=1}^{N} \prod_{\ell=\ell_{\min}}^{\ell_{\max}} \frac{1}{\sigma_\ell^i} \left(\frac{\sigma_\ell^i}{C_\ell} \right)^{\frac{2\ell+1}{2}} e^{-\frac{2\ell+1}{2}\frac{\sigma_\ell^i}{C_\ell}}, \tag{3.1}$$

   where the CMB is supposed to be distributed as a Gaussian with variance given by the power spectrum

$$C_\ell = \langle |a_{\ell m}|^2 \rangle = \frac{1}{2\ell+1} \sum_{m=-\ell}^{\ell} a_{\ell m}^* a_{\ell m}, \tag{3.2}$$

   with the CMB amplitude vector $a_{\ell m}$ defined in terms of spherical harmonics $Y_{\ell m}$,

$$\sigma_\ell^i = \frac{1}{2\ell+1} \sum_{m=-\ell}^{\ell} |a_{\ell m}^i|^2 \tag{3.3}$$

   "is the observed power spectrum of the ith Gibbs CMB sky sample, N is the total number of Gibbs samples, and $\ell_{\min}$ and $\ell_{\max}$ define the multipole range of the likelihood estimator" (p. 4). It is important to notice that this expression converges to the exact likelihood as N tends to infinity.

2. Low-ℓ polarization (EE) likelihood: This function, according to Planck Collaboration, Aghanim, N., et al. (2020a) "is built by comparing a cross-frequency power spectrum of two foreground-corrected maps to a set of simulations" (p. 2) and can be divided in two types

   (a) HFI-based low-ℓ likelihood: Following Planck Collaboration, Aghanim, N., et al. (2020a), it is based on the HFI[24] and the cross-quasi-maximum-likelihood (QLM) "spectrum of the 100 and 143 GHz maps cleaned using a template-fitting procedure from polarized synchrotron and polarized dust contaminations" (p. 7).

[23]The *Planck* Low Frequency Instrument (LFI) is a space radiometer that "observes the sky in three bands centered at 30, 44 and 70 GHz" (Bersanelli, 2023).

[24]The *Planck* High Frequency Instrument (HFI) is a space radiometer that "covers six channels between 100 and 850 GHz" (Bersanelli, 2023).

(b) LFI-based low-ℓ likelihood: It is based on the HFI and, according to Planck Collaboration, Aghanim, N., et al. (2020a), it can be written as

$$\mathcal{L}(C_\ell) = \mathcal{P}(\mathbf{m}|C_\ell) = \frac{1}{(2\pi)^{N/2}|\mathbf{M}|^{1/2}} e^{-\frac{1}{2}\mathbf{m}^T\mathbf{M}^{-1}\mathbf{m}}, \tag{3.4}$$

where $\mathcal{P}(\mathbf{m}|C_\ell)$ is the conditional probability of $\mathbf{m}$ given C_ℓ, with $\mathbf{m}$ "a foreground-mitigated temperature and linear polarization map array of total length N pixels, whose signal-plus-noise covariance matrix is $\mathbf{M}$" (p. 17). Here, the `Commander` solution described above is employed for the temperature map and the "linear polarization CMB maps are estimated from the LFI 70 GHz channel, using the 353 and 30 GHz channels as tracers to minimize the polarized dust and synchrotron emission, respectively" (p. 17).

3. High-ℓ temperature and polarization (TT, TE, and EE) likelihoods: According to Planck Collaboration, Aghanim, N., et al. (2020a), these functions consider multipoles $\ell \geq 30$ and use "multiple cross-frequency spectra estimates, assuming smooth foreground and nuisance spectra templates and a Gaussian likelihood approximation" (p. 2), "based on the three cleanest *Planck*-HFI channels, namely the 100, 143, and 217 GHz ones, [which] represent the best optimization between resolution, sensitivity, and low foreground contamination" (p. 24). These likelihoods can be written as

$$\mathcal{L}(\hat{\mathbf{C}}|\mathbf{C}(\boldsymbol{\theta})) = \exp\left(-\frac{1}{2}\left[\hat{\mathbf{C}} - \mathbf{C}(\boldsymbol{\theta})\right]^T \Sigma^{-1}\left[\hat{\mathbf{C}} - \mathbf{C}(\boldsymbol{\theta})\right] + \text{const.}\right), \tag{3.5}$$

"where $\hat{\mathbf{C}}$ is the data vector, $\mathbf{C}(\boldsymbol{\theta})$ is the prediction for the model with parameter values $\boldsymbol{\theta}$, and Σ is the covariance matrix (computed for a fiducial cosmology)" (p. 24).

Chapter 4

Results

4.1 CLASS test

The CLASS code is tested in the background using Python and considering as a base the best-fit cosmological parameter values of Planck Collaboration, Aghanim, N., et al. (2020b). First, it is tested without considering the PBH model, to see if it works properly. Then, considering that all dark matter consist of PBHs (that is, $f_{\mathrm{PBH}} = 1$). And, finally, searching for the lowest possible initial masses of PBHs before complete evaporation, finding $M_{\mathrm{in}} = 6.46 \times 10^{14}\,\mathrm{g}$, independently of f_{PBH} value. The CLASS code test is explained in detail in Appendix C.

4.2 The cosmological parameters for the PBH model

The cosmological parameters are estimated considering the PBH model and using Markov chain Monte Carlo methods, first with a maximum limit of samples and then without constraining its number. For this, the *Planck* data and CMB likelihood functions are used; specifically, low-ℓ and high-ℓ temperature and polarization likelihoods (see the CMB maps and the *Planck* CMB likelihoods sections for more details), installed with the Cobaya package, which is used for MCMC sampling in Python. Due to the high computational complexity of doing this (because of the large amount of data and parameters considered), the author used the resources of the National Energy Research Scientific Computing Center (NERSC). Specifically, the login node is used, which consists of 15 nodes and two sockets of AMD EPYC 7742 (Rome) processors[25] with 64 CPU cores per sockets and 512 GB of memory in total.

Before taking the PBH model into account and limiting MCMC to 10 000 samples, the cosmological parameters are estimated considering only the ΛCDM model, finding $H_0 = 67.3 \pm 0.6\,\mathrm{km\,s^{-1}\,Mpc^{-1}}$, $\Omega_{m,0} = 0.315 \pm 0.008$, $\Omega_{b,0}h^2 = 0.022\,27 \pm 0.000\,15$, $\Omega_{c,0}h^2 = 0.1198 \pm 0.0014$ and $\Omega_{\Lambda,0} = 0.685 \pm 0.008$ as best-fit parameters, with $\chi^2_{\mathrm{min}} = 2762.82$; taking 14 hours; and plotting the 68 % and 95 % confidence contours (see Figure 4.1).

[25] For more information, see https://www.amd.com/en/products/cpu/amd-epyc-7742.

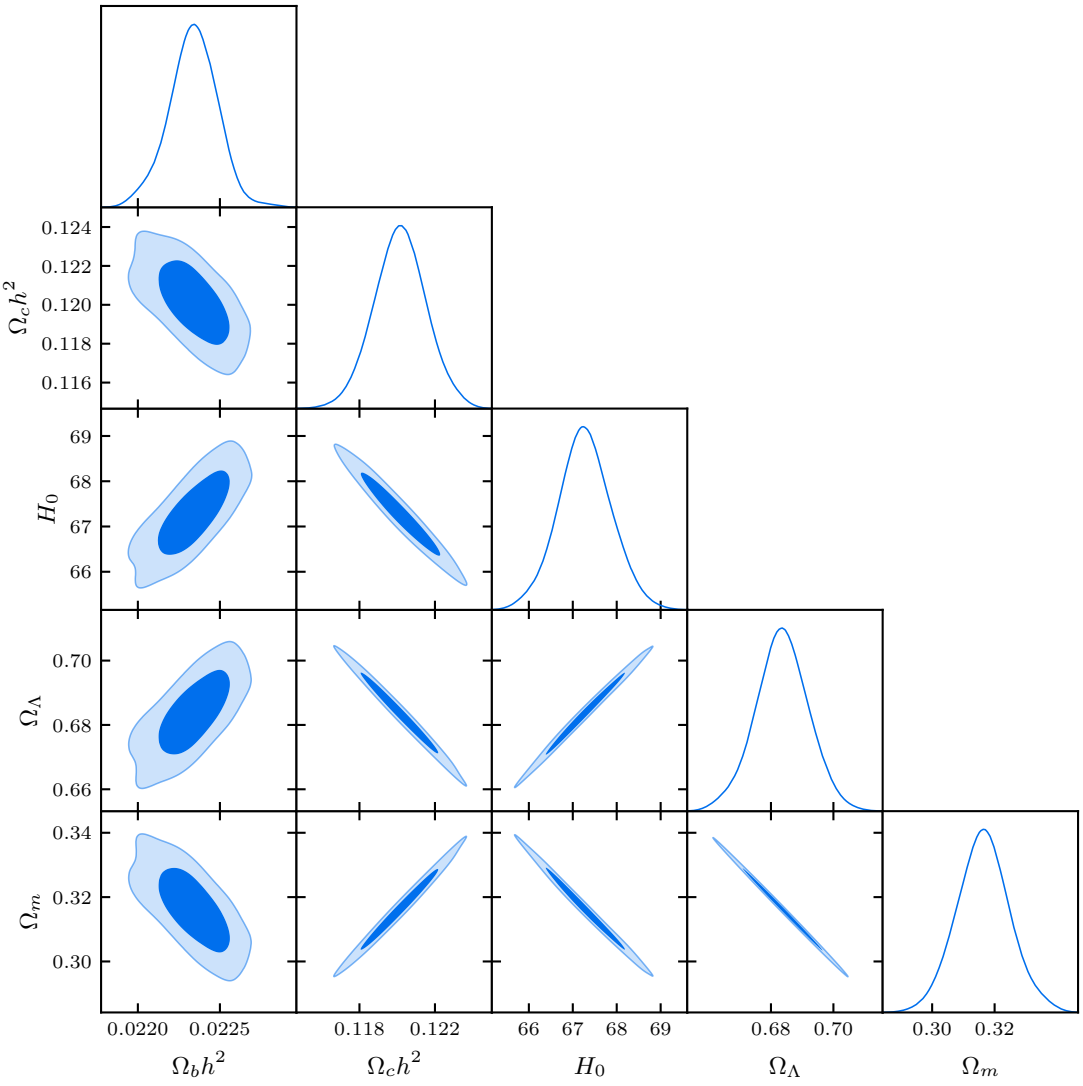

Figure 4.1: The 68 % and 95 % confidence contours for the ΛCDM model, limited to 10 000 samples.

4.2.1 Limited estimation

To test if the code can estimate the cosmological parameters considering the PBH model, these are estimated first with MCMC limited to 10 000 samples (or accepted steps). For this, two cases are considered. In the first one, following Planck Collaboration, Aghanim, N., et al. (2020b) to fix $\Omega_{\Lambda,0} = 0.6842$, the cosmological parameters are estimated, finding $H_0 = 67.3 \pm 0.5\,\mathrm{km\,s^{-1}\,Mpc^{-1}}$, $\Omega_{m,0} = 0.316 \pm 0.006$, $\Omega_{b,0}h^2 = 0.022\,31 \pm 0.000\,14$, $\Omega_{c,0}h^2 = 0.1202 \pm 0.0011$, $f_{\mathrm{PBH}} = 0.001\,65 \pm 0.004\,33$ and $\log(\tilde{\alpha}) = -8.1959 \pm 6.5685$ ($M_{\mathrm{in}} = 2.46 \times 10^{17}\,\mathrm{g}$) as best-fit parameters, with $\chi^2_{\mathrm{min}} = 2766.11$; taking 15 hours; and plotting the 68 % and 95 % confidence contours (see Figure 6.10 in Appendix D).

On the other hand, in the second case, without setting any cosmological parameter, the best fits are $H_0 = 67.1 \pm 0.6\,\mathrm{km\,s^{-1}\,Mpc^{-1}}$, $\Omega_{m,0} = 0.319 \pm 0.008$, $\Omega_{b,0}h^2 = 0.022\,23 \pm 0.000\,13$, $\Omega_{c,0}h^2 = 0.1205 \pm 0.0013$, $\Omega_{\Lambda,0} = 0.681 \pm 0.008$, $f_{\mathrm{PBH}} = 0.001\,52 \pm 0.001\,91$ and $\log(\tilde{\alpha}) =$

-19.5678 ± 5.9543 ($M_{\rm in} = 1.52 \times 10^{21}$ g), with $\chi^2_{\rm min} = 2765.51$; taking 15 hours; and the 68 % and 95 % confidence contours are plotted in Appendix D (see Figure 6.11).

4.2.2 Unlimited estimation

Here, several cases are considered to estimate the cosmological parameters, limited only by Gelman-Rubin statistic on means $R_{\rm min} - 1 = 0.01$. In the first one, following Planck Collaboration, Aghanim, N., et al. (2020b) to fix $\Omega_{\Lambda,0} = 0.6842$, the best-fit cosmological parameters are $H_0 = 67.2 \pm 0.6\,{\rm km\,s^{-1}\,Mpc^{-1}}$, $\Omega_{m,0} = 0.317 \pm 0.008$, $\Omega_{b,0}h^2 = 0.022\,33 \pm 0.000\,15$, $\Omega_{c,0}h^2 = 0.1204 \pm 0.0014$, $f_{\rm PBH} = 0.000\,58 \pm 0.001\,87$ and $\log(\tilde{\alpha}) = -11.4828 \pm 6.5496$ ($M_{\rm in} = 3.06 \times 10^{18}$ g), with $\chi^2_{\rm min} = 2764.32$; taking 6 days and 23 hours; and the 68 % and 95 % confidence contours are plotted in Figure 4.2.

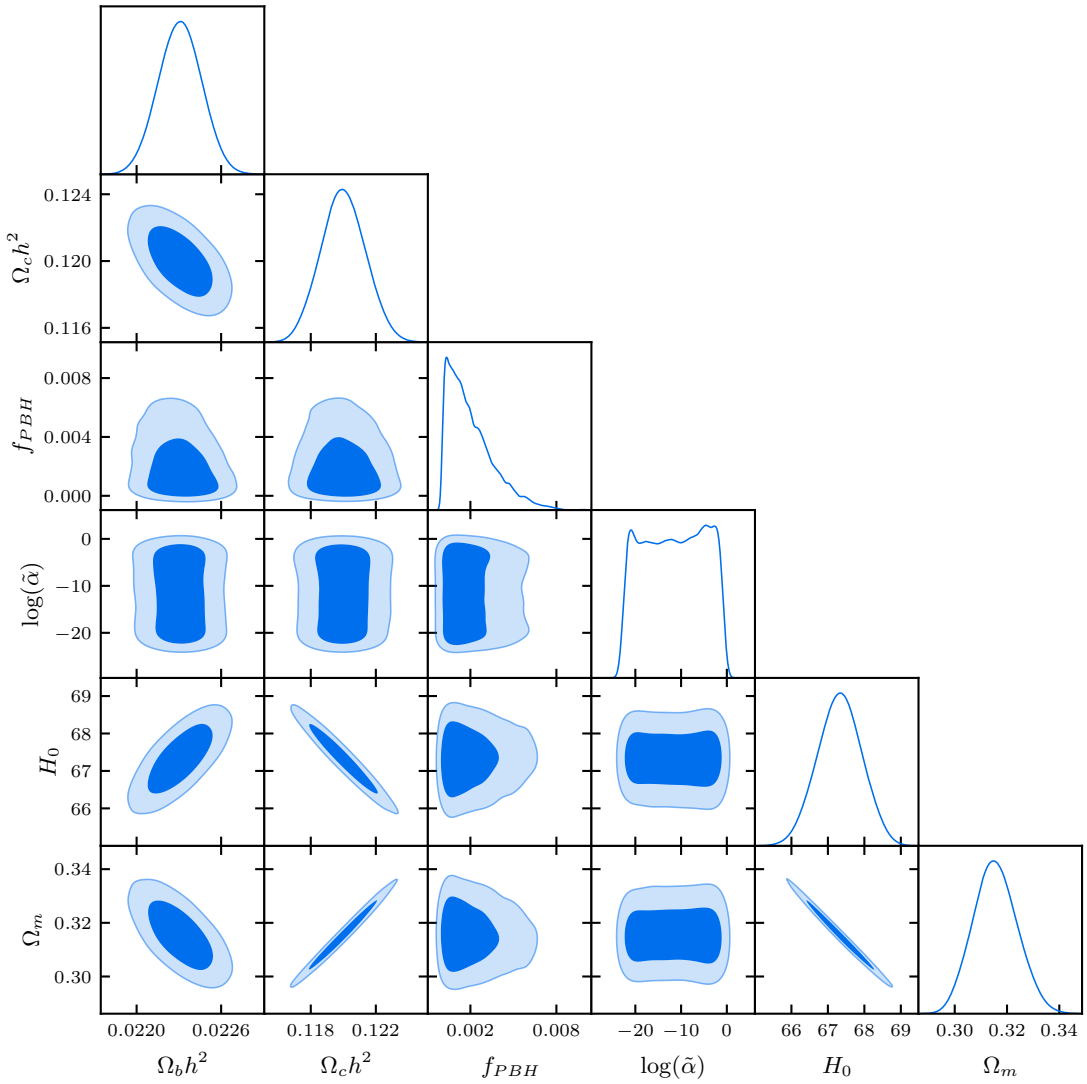

Figure 4.2: The 68 % and 95 % confidence contours for the PBH model, with $\Omega_{\Lambda,0} = 0.6842$ fixed.

In the second case, without setting any cosmological parameter, they are estimated, finding $H_0 = 67.6 \pm 0.6\,\mathrm{km\,s^{-1}\,Mpc^{-1}}$, $\Omega_{m,0} = 0.312 \pm 0.008$, $\Omega_{b,0}h^2 = 0.022\,39 \pm 0.000\,15$, $\Omega_{c,0}h^2 = 0.1196 \pm 0.0014$, $\Omega_{\Lambda,0} = 0.688 \pm 0.008$, $f_{\mathrm{PBH}} = 0.000\,75 \pm 0.001\,68$ and $\log(\tilde{\alpha}) = -6.3433 \pm 5.7478$ ($M_{\mathrm{in}} = 6.92 \times 10^{16}\,\mathrm{g}$) as best-fit parameters, with $\chi^2_{\mathrm{min}} = 2764.76$; taking 3 days and 18 hours; and plotting the 68 % and 95 % confidence contours in Figure 4.3.

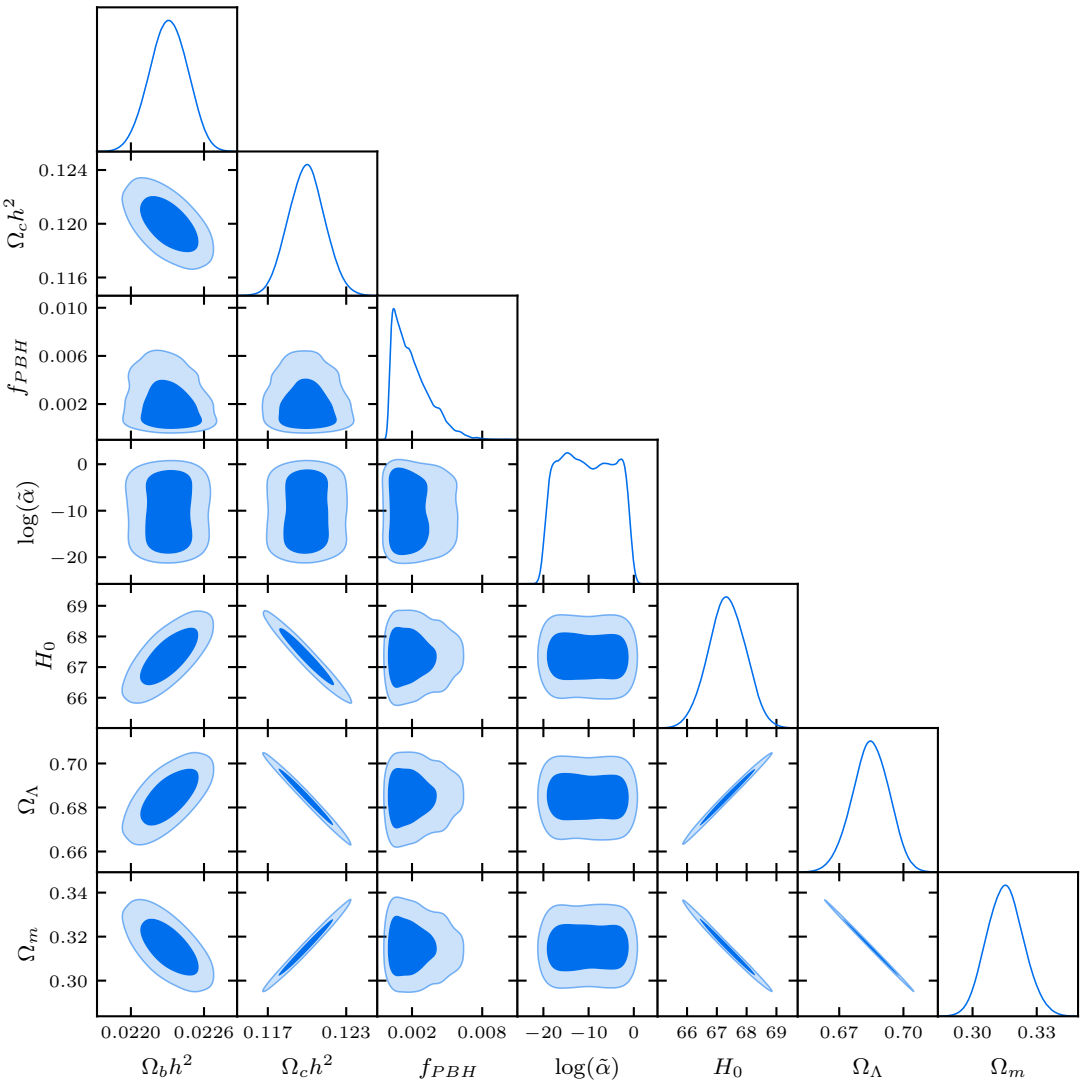

Figure 4.3: The 68 % and 95 % confidence contours for the PBH model.

In the third case, constraining $f_{\rm PBH}$ to be greater than 0.1 and $-23 < \log(\tilde{\alpha}) < -6$ ($10^{17}\,{\rm g} \lesssim M_{\rm in} \lesssim 10^{22}\,{\rm g}$ in terms of the initial PBH mass), the best-fit parameters are $H_0 = 72.9 \pm 1.0\,{\rm km\,s^{-1}\,Mpc^{-1}}$, $\Omega_{m,0} = 0.239 \pm 0.012$, $\Omega_{b,0}h^2 = 0.021\,25 \pm 0.000\,28$, $\Omega_{c,0}h^2 = 0.1056 \pm 0.0025$, $\Omega_{\Lambda,0} = 0.760 \pm 0.012$, $f_{\rm PBH} = 0.100\,11 \pm 0.000\,31$ and $\log(\tilde{\alpha}) = -20.1620 \pm 4.7933$ ($M_{\rm in} = 2.33 \times 10^{21}\,{\rm g}$), with $\chi^2_{\rm min} = 3280.01$; taking 7 days and 7 hours; and the 68 % and 95 % confidence contours are plotted in Figure 4.4.

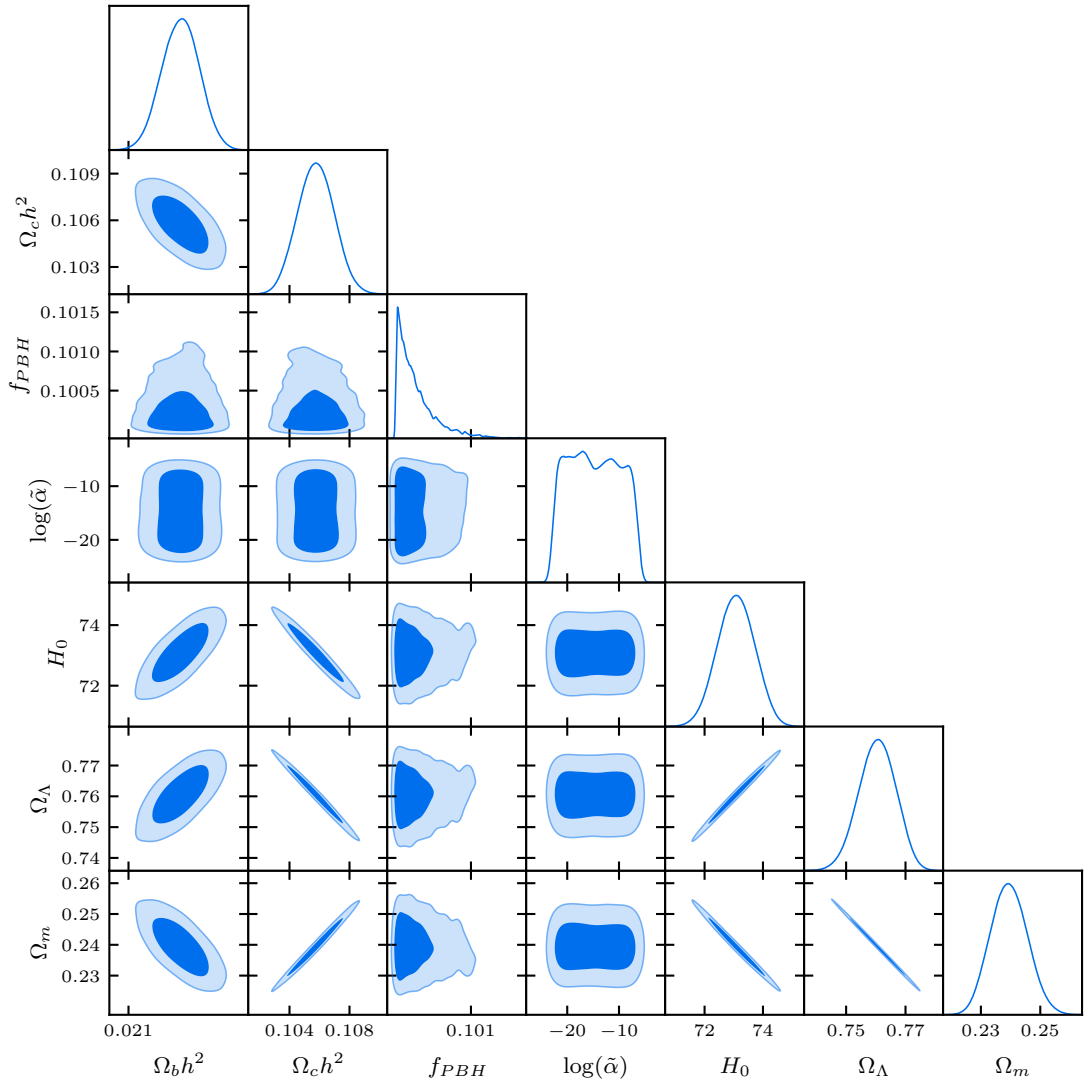

Figure 4.4: The 68 % and 95 % confidence contours for the PBH model, with $f_{\rm PBH} > 0.1$ and $-23 < \log(\tilde{\alpha}) < -6$.

Finally, in the fourth case, constraining $\log(\tilde{\alpha}) = -0.455$ such that $M_{\rm in} = 6.46 \times 10^{14}\,\mathrm{g}$ is the smallest possible mass before PBH complete evaporation (independently of $f_{\rm PBH}$), the best-fit parameters are $H_0 = 67.4 \pm 0.6\,\mathrm{km\,s^{-1}\,Mpc^{-1}}$, $\Omega_{m,0} = 0.314 \pm 0.019$, $\Omega_{b,0}h^2 = 0.022\,23 \pm 0.000\,16$, $\Omega_{c,0}h^2 = 0.1198 \pm 0.0014$, $\Omega_{\Lambda,0} = 0.686 \pm 0.009$ and $f_{\rm PBH} = 0.000\,01 \pm 0.001\,77$, with $\chi^2_{\rm min} = 2764.35$; taking 7 days and 6 hours; and the 68 % and 95 % confidence contours are plotted in Figure 4.5.

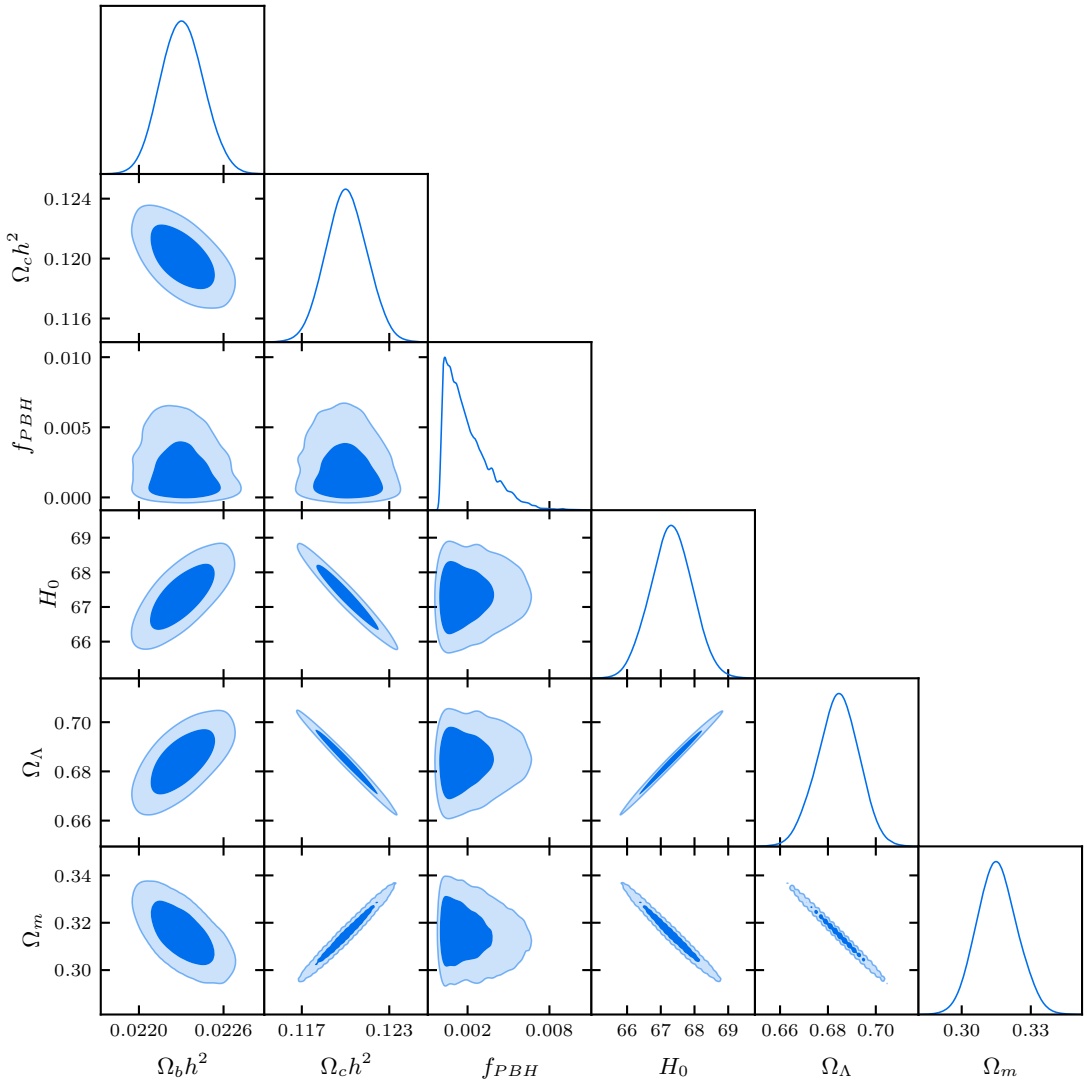

Figure 4.5: The 68 % and 95 % confidence contours for the PBH model, with $\log(\tilde{\alpha}) = -0.455$.

A summary of the results is shown in Table 4.1, which illustrates the best-fit parameters for the ΛCDM model, comparing the results obtained by the author with those by Planck Collaboration, Aghanim, N., et al. (2020b); and the best-fit parameters for the PBH model in the four cases considered by the author and Nesseris et al. (2020) article.

Table 4.1: Best-fit parameters for the ΛCDM and the PBH model in the cases considered by the author and Nesseris et al. (2020) article.

ΛCDM	*Planck*	Author		
h	0.673 ± 0.012	0.673 ± 0.006		
$\Omega_{m,0}$	$0.317^{+0.017}_{-0.016}$	0.315 ± 0.008		
$\Omega_{b,0}h^2$	$0.022\,36 \pm 0.000\,29$	$0.022\,27 \pm 0.000\,15$		
$\Omega_{c,0}h^2$	0.1202 ± 0.0027	0.1198 ± 0.0014		
$\Omega_{\Lambda,0}$	$0.683^{+0.016}_{-0.017}$	0.685 ± 0.008		
$\chi^2_{\min}$	2764.0	2762.82		
PBH (author)	$\Omega_{\Lambda,0} = 0.6842$	All free	$f_{\rm PBH} > 0.1$	$\log(\tilde{\alpha}) = -0.455$
h	0.672 ± 0.006	0.676 ± 0.006	0.729 ± 0.010	0.674 ± 0.006
$\Omega_{m,0}$	0.317 ± 0.008	0.312 ± 0.008	0.239 ± 0.012	0.314 ± 0.019
$\Omega_{b,0}h^2$	$0.022\,33 \pm 0.000\,15$	$0.022\,39 \pm 0.000\,15$	$0.021\,25 \pm 0.000\,28$	$0.022\,23 \pm 0.000\,16$
$\Omega_{c,0}h^2$	0.1204 ± 0.0014	0.1196 ± 0.0014	0.1056 ± 0.0025	0.1198 ± 0.0014
$\Omega_{\Lambda,0}$	–	0.688 ± 0.008	0.760 ± 0.012	0.686 ± 0.009
$f_{\rm PBH}$	$0.000\,58 \pm 0.001\,87$	$0.000\,75 \pm 0.001\,68$	$0.100\,11 \pm 0.000\,31$	$0.000\,01 \pm 0.001\,77$
$\log(\tilde{\alpha})$	-11.4828 ± 6.5496	-6.3433 ± 5.7478	-20.1620 ± 4.7933	–
$\chi^2_{\min}$	2764.32	2764.76	3280.01	2764.35
PBH (article)	All free	$f_{\rm PBH} = 1$ $\log(\tilde{\alpha}) = -4$		
h	0.654 ± 0.019	0.654 ± 0.017		
$\Omega_{b,0}h^2$	$0.022\,22 \pm 0.002\,25$	$0.022\,25 \pm 0.002\,20$		
$\Omega_{c,0}h^2$	0.1197 ± 0.0129	0.1194 ± 0.0129		
$f_{\rm PBH}$	0.8768 ± 11.9041	–		
$\log(\tilde{\alpha})$	-10.1349 ± 5.6832	–		

Chapter 5

General discussion

5.1 Difficulties with the CAMB code

The Code for Anisotropies in the Microwave Background (CAMB) (Lewis et al., 2000) "is a cosmology code for calculating cosmological observables, including CMB, lensing, source count and 21cm angular power spectra, matter power spectra, transfer functions and background evolution, ... [written] in Python, with numerical code implemented in fast modern Fortran" (Lewis & Challinor, 2023).

The main advantage of using CAMB is that the background dynamical equations are written in terms of the conformal time τ, which solves the problem of the Hubble parameter (see the CLASS code section) because it does not appear in the dynamical equations for PBHs and its associated dark radiation

$$\frac{d\tilde{\Omega}_{\rm PBH}}{d\tau} = -\frac{a\tilde{\alpha}\left(f_{\rm PBH}\Omega_{c,0}\right)^3}{\tilde{\Omega}_{\rm PBH}^2}, \tag{5.1a}$$

$$\frac{d\tilde{\Omega}_X}{d\tau} = \frac{a^{1+3w_X}\tilde{\alpha}\left(f_{\rm PBH}\Omega_{c,0}\right)^3}{\tilde{\Omega}_{\rm PBH}^2}. \tag{5.1b}$$

Initially, considering this important advantage, the CAMB code was used by the author, following Li and Zhang's (2023) coupled field model to adapt it to the PBH model. The numerical routine IDECAMB published by Li and Zhang (2023) implements Interacting Dark Energy (IDE) scenery in CAMB, allowing dark energy and matter to interact with each other. However, after two months trying to verify if IDECAMB works with CAMB and modifying it, one of the authors of IDECAMB notified that it only works with 2018's outdated version of CAMB.

Considering the complexity of editing CAMB from nothing, added to the time limitation and that in the CLASS code interacting dark energy is already implemented and working, the author decided to migrate to the last one and adapt it to the PBH model.

5.2 CLASS test

Before estimating the cosmological parameters, the CLASS code was tested in the background using Python and the results can be seen in Chapter 4. It works well when considering large initial PBH masses (above 6.46×10^{14} g) or low values for $\tilde{\alpha}$ (lower than $10^{-0.455}$). In these cases, the PBH evaporates and the associated dark radiation raises according to theory.

The problem of considering initial PBH masses lower than 6.46×10^{14} g is that PBH evaporates completely before a = 1 (independently of f_{PBH}), thus the dynamical equations diverge and it has to be imposed that if the equation diverges, $\Omega_{\mathrm{PBH}} = 0$. The difficulty on doing this is that Ω_X is not equal to zero; it has to raise and then decrease at some unknown rate. Since for dark radiation $\Omega_X \sim a^{-3(1+w_X)}$, it is natural to think, based on equation (2.7) that, after the time a^* when $\Omega_{\mathrm{PBH}} = 0$, $\Omega_X = \Omega_X^*(a/a^*)^{-3(1+w_X)}$, where Ω_X^* is Ω_X when $a = a^*$. However, this proposal did not solve the problem. If it is considered, the obtained radiation after the PBH complete evaporation is lower than expected, in other words, dark radiation decreases faster than expected after the PBH evaporates completely. This may be because w_X is not always necessarily equal to 1/3, as in *common* radiation. An interesting future work could be solving this problem to reduce the Hubble tension by considering lower PBH initial masses.

5.3 The cosmological parameters for the PBH model

The cosmological parameters were estimated for the PBH model using MCMC methods in Python, considering first a maximum limit of accepted steps and then without this constrain. For this, the *Planck* data and low-ℓ and high-ℓ temperature and polarization CMB likelihood functions were used[26]. Also, it is necessary to highlight that all the parameters concerning the ΛCDM model were estimated, but only the most significant ones will be discussed, that is, those that appear in the first Friedmann equation for the PBH model (see equation (2.21)).

But, before estimating the cosmological parameters for the PBH model, to test if the Cobaya package works well, only the ΛCDM model was considered and, with a limit of 10 000 samples for MCMC, its associated parameters were estimated, showing them in Table 4.1 and plotting the 68 % and 95 % confidence contours in Figure 4.1. It can be seen that the results obtained by the author are very similar to those of *Planck*, but they are also improved, finding a lower associated error and χ^2_{min} than *Planck*. This test shows that the code works well for ΛCDM alone and allows checking if it can run properly for the PBH model.

5.3.1 Limited estimation

Considering a maximum limit of 10 000 samples for MCMC, the cosmological parameters were estimated in two different cases to test if the code works for the PBH model. In the first one, with $\Omega_{\Lambda,0} = 0.6842$ fixed according to Planck Collaboration, Aghanim, N., et al.

[26] A detailed explanation of these can be found in the CMB maps and the *Planck* CMB likelihoods sections.

(2020b), the estimated values, shown in the limited estimation results' section, are similar to the ΛCDM model, with values for H_0 and $\Omega_{c,0}h^2$ coinciding exactly with *Planck* results, except for the associated errors, which are lower in the author's best-fit. Despite this, the minimum χ^2 is larger than in *Planck*, but this is expected since convergence has not been reached due to the imposed sampling limit, which can be seen in Figure 6.10 ($\tilde{\alpha}$ seems unconstrained due to the shape of the confidence region).

In the second case, without setting any cosmological parameter, the estimated values, shown in the limited estimation results' section, are also similar to the ΛCDM model, but none of them coincide exactly with *Planck* results. The minimum χ^2 is larger than *Planck*'s but lower than when $\Omega_{\Lambda,0}$ is fixed. However, since convergence has not been reached due to the imposed sampling limit (see the confidence region's shape of $f_{\rm PBH}$ and $\tilde{\alpha}$ in Figure 6.11), it is not necessarily a best model than the previous case to explain the Universe.

These two cases show that the code works well for the PBH model, allowing estimating the cosmological parameters without constraining the number of samples.

5.3.2 Unlimited estimation

After testing successfully that the code works for the ΛCDM and PBH models, four cases of interest were considered to estimate the cosmological parameters for the PBH model using MCMC methods, limiting it only by Gelman-Rubin statistic on means $R_{\rm min} - 1 = 0.01$, to avoid unnecessary sampling.

Firstly, setting $\Omega_{\Lambda,0} = 0.6842$ as in the first limited estimation case, the cosmological parameters were estimated and are shown in Table 4.1, finding similar values to the ΛCDM model, where $\Omega_{m,0}$ coincides exactly with *Planck* results, except for the associated errors, which are lower in the author's best fits. They are also similar to Nesseris et al. (2020) estimated parameters, differing significatively only in H_0 and $f_{\rm PBH}$. This similar results between ΛCDM and PBH implies that the associated dark radiation to PBH evaporation does not affect the Universe's expansion rate. The minimum χ^2 is lower than in the limited estimation case, but higher than ΛCDM in both *Planck* and author's results, as expected since convergence has been achieved (see Figure 4.2) and the ΛCDM model has fewer parameters than the PBH one.

Secondly, without constraining the cosmological parameters, they were estimated and are shown in Table 4.1. It can be seen that the best fits obtained by the author are similar to those of *Planck*, even though none of them match exactly, as in the previous case; implying that the PBH associated dark radiation due to its evaporation does not change the Universe's expansion. The associated errors are small and the minimum χ^2 is larger than in the previous case and in both *Planck* and author's results for ΛCDM, as expected since here all the parameters are free and are more than in the ΛCDM model. As shown in Figure 4.3, convergence has been achieved, so $\chi^2_{\rm min}$ is lower than in the limited estimation case.

Thirdly, trying to explain the largest possible amount of dark matter, the cosmological parameters were estimated constraining $f_{\rm PBH} > 0.1$ and $10^{17}\,{\rm g} \lesssim M_{\rm in} \lesssim 10^{22}\,{\rm g}$, the maximum lower limit for the fraction of PBHs that is supported by the code when running MCMC. The

best fits are shown in Table 4.1 and it can be seen that, surprisingly, they are very different from the previous cases for the PBH model and even from ΛCDM alone. Here, the Hubble constant raises from $67.3 \pm 1.2\,\mathrm{km\,s^{-1}\,Mpc^{-1}}$ (in *Planck*'s case) to $72.9 \pm 1.0\,\mathrm{km\,s^{-1}\,Mpc^{-1}}$, being also higher than $70.5 \pm 1.3\,\mathrm{km\,s^{-1}\,Mpc^{-1}}$, the best fit found by Nesseris et al. (2020) when considering an ultra-light PBH fraction ($f_{\mathrm{PBH}} = 10^{-7}$ and $M_{\mathrm{in}} = 10^{9}\,\mathrm{g}$), despite finding $M_{\mathrm{in}} = 2.33 \times 10^{21}\,\mathrm{g}$ as the best fit by the author, a large mass to have a considerable contribution of dark radiation to the energy budget. Remarkably, the value for H_0 found by the author coincides exactly with Dhungana et al. (2023) estimation using observations of type IIP supernovae[27], which could help to reduce the tension. Another surprising result is that the best fit for matter and dark energy is, respectively, too low and high when compared with the previous cases, including the ΛCDM model. This could lead to a raise in the acceleration of the Universe's expansion. The associated errors and the minimum χ^2 are higher than in the previous cases for PBH, probably implying that the code does not bear well imposing $f_{\mathrm{PBH}} > 0.1$, namely a large amount of dark matter explained by PBHs. It has to be noticed that convergence has not been achieved for f_{PBH}, as seen in its confidence region's shape in Figure 4.4, affecting the best-fit parameters, but probably not considerably.

Finally, in the fourth case, the author tries to explain the discrepancy between the CMB and the local measurements of H_0 by considering the lightest possible PBH before complete evaporation. According to the `CLASS` code test, its lowest initial mass is $M_{\mathrm{in}} = 6.46 \times 10^{14}\,\mathrm{g}$, independently of f_{PBH}. Thus, $\log(\tilde{\alpha}) = -0.455$ is fixed such that $M_{\mathrm{in}} = 6.46 \times 10^{14}\,\mathrm{g}$, for estimating the cosmological parameters, whose best fits are shown in Table 4.1. However, the results do not change too much from the ΛCDM model and H_0 increases a little compared to it and the first case, but it is lower than in the second case, when all the parameters are free. This could imply that the initial mass is not low enough to have a considerable dark radiation contribution and raise the Hubble constant. As discussed previously, in future works the equation of state parameter of dark radiation w_X value can be adjusted to account for the necessary amount of radiation to raise H_0 and solve the Hubble tension problem. The best fit associated errors and the minimum χ^2 are similar to the first two cases, being lower than the third one, and convergence has been achieved, which can be seen in Figure 4.5.

[27] A supernova is the result of the explosion of certain types of stars. In particular, the progenitor of a Type IIP supernova is a red supergiant star whose core collapses at the end of its life, where the P comes from the characteristic plateau of its light curve (Carroll & Ostlie, 2017).

Chapter 6

Conclusions

Primordial black holes could be the key to unveiling the mysteries of the nature of dark matter and the Hubble tension. In this work, continuing Nesseris et al.'s (2020) by assuming that a fraction of the Universe's dark matter consists of PBHs, the cosmological parameters are estimated using MCMC methods, seeking to verify if the PBH model fits reality and helps to understand the nature of DM and reduce the Hubble tension. The novelty concerning Nesseris et al. (2020) article is that here, all the *Planck* data and its CMB likelihoods are used, looking for more accurate results.

Initially, the `CAMB` code was used, trying to adapt it to the PBH model, considering its advantage solving the problem of the Hubble parameter in the dynamical equations for PBHs and dark radiation, but, due to the complexity of modifying it, `CLASS` was preferred for its friendliness, flexibility, accuracy and speed, despite the dependency of the Hubble parameter in the mentioned equations.

Using `CLASS`, the cosmological parameters were estimated considering several cases in the results chapter, and analyzed and commented in detail in the general discussion chapter. An interesting finding is that the author's best fits for the ΛCDM coincide with *Planck*'s, but with associated errors even lower. Also, when considering all the parameters free, $\Omega_{\Lambda,0} = 0.6842$ or $M_{\text{in}} = 6.46 \times 10^{14}\,\text{g}$ fixed for the PBH model, the obtained results are very similar to ΛCDM. Where, as expected, the first one is the case with the lowest χ^2_{min} since it has $\Omega_{\Lambda,0}$ settled as *Planck*'s best fit; but if the priors $f_{\text{PBH}} > 0.1$ and $10^{17}\,\text{g} \lesssim M_{\text{in}} \lesssim 10^{22}\,\text{g}$ are considered (trying to explain the amount of dark matter as much as possible through the code), the Hubble constant surprisingly raises to $72.9 \pm 1.0\,\text{km}\,\text{s}^{-1}\,\text{Mpc}^{-1}$, being also higher than in the article of Nesseris et al. (2020), but coinciding exactly with the estimation of Dhungana et al. (2023) using observations of core-collapse supernovae; helping to reduce the Hubble tension. In this case, the matter and dark energy's best fit is also different from ΛCDM, causing the acceleration of the Universe's expansion to increase.

The first two cases (when $\Omega_{\Lambda,0} = 0.6842$ is fixed and when all parameters are free) serve to explain only a small amount of dark matter, since the fraction of PBHs are $0.000\,58 \pm 0.001\,87$ and $0.000\,75 \pm 0.001\,68$, respectively. With the third case, the author tried to explain more of it, but finds the unexpected results described in the previous paragraph, reducing the Hubble tension but getting parameters that differ considerably from the known Universe. Finally,

in the fourth case, it is expected to reduce the tension, but H_0 only raises a little compared with ΛCDM.

An interesting insight is that the best-fit parameters obtained by the author for the PBH model fit ΛCDM better than Nesseris et al. (2020) ones. This can be explained by the use of all the *Planck* data and its CMB likelihood functions, instead of an approximation.

Several ongoing and planned experiments will test the hypothesis of PBH as a dark matter candidate. Among them are Euclid, a wide-angle space telescope developed by the European Space Agency (ESA) and the Euclid Consortium launched on July 1st, 2023, and designed to explore the composition and evolution of the dark Universe, which would help to understand better the nature of dark matter; and the James Webb Space Telescope (JWST), an orbiting infrared observatory developed by the National Aeronautics and Space Administration (NASA), the ESA and the Canadian Space Agency (CSA) launched on December 25th, 2021, and designed to complement and extend the Hubble Space Telescope's discoveries, for example, improving the precision of the Hubble parameter local measurements, which would help to reduce the tension.

As future work, `CLASS` calculations of the background could be modified by taking the PBH dynamical equations with respect to the conformal time and not the scale factor. This change avoids biasing the PBH model assuming the ΛCDM's Hubble parameter. Also, it would be interesting to solve the dark radiation problem after PBH complete evaporation, accounting for the necessary amount of radiation to raise the Hubble constant, seeking the reduction of its tension. Finally, extended mass functions for PBHs and perturbation theory (which are not taken into account for simplicity) could be considered in future research, ensuring that the model used fits closer to reality.

Bibliography

Abbott, B. P., Abbott, R., Abbott, T. D., Abernathy, M. R., Acernese, F., Ackley, K., Adams, C., Adams, T., Addesso, P., Adhikari, R. X., Adya, V. B., Affeldt, C., Agathos, M., Agatsuma, K., Aggarwal, N., Aguiar, O. D., Aiello, L., Ain, A., Ajith, P., ... Zweizig, J. (2016). Observation of Gravitational Waves from a Binary Black Hole Merger. *Physical Review Letters*, *116*, 061102. https://doi.org/10.1103/PhysRevLett.116.061102

Akaike, H. (1974). A New Look at the Statistical Model Identification. *IEEE Transactions on Automatic Control*, *19*, 716-723. http://doi.org/10.1109/tac.1974.1100705

Amendola, L., & Tsujikawa, S. (2010). *Dark Energy: Theory and Observations* (1st ed.). Cambridge: Cambridge University Press. https://doi.org/10.1017/CBO9780511750823

Arbey, A., & Mahmoudi, F. (2021). Dark matter and the early Universe: A review. *Progress in Particle and Nuclear Physics*, *119*, 103865. https://doi.org/10.1016/j.ppnp.2021.103865

Audren, B. (2014). *Python wrapper.* https://github.com/lesgourg/class_public/wiki/Python-wrapper (Accessed: 2023-11-22)

Bayes, T., & Price, R. (1763). An essay towards solving a problem in the doctrine of chances. *Philosophical Transactions of the Royal Society*, *53*, 370–418. https://doi.org/10.1098/rstl.1763.0053

Bersanelli, M. (2023). *The Planck Low Frequency Instrument.* https://iopscience.iop.org/journal/1748-0221/page/extra.proc5 (Accessed: 2023-10-19)

Blas, D., Lesgourgues, J., & Tram, T. (2011). The Cosmic Linear Anisotropy Solving System (CLASS). Part II: Approximation schemes. *Journal of Cosmology and Astroparticle Physics*, *2011*(07), 034. https://doi.org/10.1088/1475-7516/2011/07/034

Carr, B. J., & Hawking, S. W. (1974). Black Holes in the Early Universe. *Monthly Notices of the Royal Astronomical Society*, *168*(2), 399-415. https://doi.org/10.1093/mnras/168.2.399

Carr, B. J., Kohri, K., Sendouda, Y., & Yokoyama, J. (2021). Constraints on primordial black holes. *Reports on Progress in Physics*, *84*(11), 116902. https://doi.org/10.1088/1361-6633/ac1e31

Carr, B. J., & Kühnel, F. (2020). Primordial Black Holes as Dark Matter: Recent Developments. *Annual Review of Nuclear and Particle Science*, *70*(1), 355-394. https://doi.org/10.1146/annurev-nucl-050520-125911

Carr, B. J., Kühnel, F., & Sandstad, M. (2016). Primordial black holes as dark matter. *Physical Review D*, *94*, 083504. https://doi.org/10.1103/PhysRevD.94.083504

Carr, B. J., & Kühnel, F. (2021). Primordial Black Holes as Dark Matter Candidates. *arXiv e-prints*. https://doi.org/10.48550/arXiv.2110.02821

Carroll, B. W., & Ostlie, D. A. (2017). *An Introduction to Modern Astrophysics* (2nd ed.). Cambridge: Cambridge University Press. https://doi.org/10.1017/9781108380980

Cheek, A., Heurtier, L., Perez-Gonzalez, Y. F., & Turner, J. (2023). Evaporation of primordial black holes in the early Universe: Mass and spin distributions. *Physical Review D*, *108*, 015005. https://doi.org/10.1103/PhysRevD.108.015005

Dhungana, G., Kehoe, R., Staten, R., Vinko, J., Wheeler, J. C., Akerlof, C. W., Doss, D., Farrente, F. V., Gibson, C. A., Lasker, J., Marion, G. H., Bhushan Pandey, S., Quimby, R., Rykoff, E., Smith, D. A., Yuan, F., & Zheng, W. (2023). Cosmological Distance Measurement of 12 Nearby Supernovae IIP with ROTSE-IIIB. *arXiv e-prints*. https://doi.org/10.48550/arXiv.2308.00916

Ding, Q. (2023). The merger rate of primordial black hole binaries as a probe of Hubble parameter. *arXiv e-prints*. https://doi.org/10.48550/arXiv.2312.13728

Dodelson, S. (2003). *Modern Cosmology* (1st ed.). Academic Press, Elsevier Science.

Einstein, A. (1915). *On the General Theory of Relativity* (1st ed.). Berlin: Sitzungsber. Preuss. Akad. Wiss.

Escrivà, A., Kuhnel, F., & Tada, Y. (2022). Primordial Black Holes. *arXiv e-prints*. https://doi.org/10.48550/arXiv.2211.05767

Gelman, A., Carlin, J., Stern, H., Dunson, D., Vehtari, A., & Rubin, D. (2021). *Bayesian Data Analysis* (3rd ed.).

Gelman, A., & Rubin, D. B. (1992). Inference from Iterative Simulation Using Multiple Sequences. *Statistical Science*, *7*(4), 457-472. https://doi.org/10.1214/ss/1177011136

Green, A. M., & Kavanagh, B. J. (2021). Primordial black holes as a dark matter candidate. *Journal of Physics G: Nuclear and Particle Physics*, *48*(4), 043001. https://doi.org/10.1088/1361-6471/abc534

Górski, K. M., Hivon, E., Banday, A. J., Wandelt, B. D., Hansen, F. K., Reinecke, M., & Bartelmann, M. (2005). HEALPix: A Framework for High-Resolution Discretization and Fast Analysis of Data Distributed on the Sphere. *The Astrophysical Journal*, *622*(2), 759. https://doi.org/10.1086/427976

Hawking, S. W. (1971). Gravitationally Collapsed Objects of Very Low Mass. *Monthly Notices of the Royal Astronomical Society*, *152*(1), 75-78. https://doi.org/10.1093/mnras/152.1.75

Hawking, S. W. (1974). Black hole explosions? *Nature*, *248*(5443), 30-31. https://doi.org/10.1038/248030a0

Hawking, S. W. (1975). Particle creation by black holes. *Communications in Mathematical Physics*, *43*(3), 199-220. https://doi.org/10.1007/BF02345020

Heavens, A. (2009). Statistical techniques in cosmology. *arXiv e-prints*. https://doi.org/10.48550/arXiv.0906.0664

Hu, J.-P., & Wang, F.-Y. (2023). Hubble Tension: The Evidence of New Physics. *Universe*, *9*(2). https://doi.org/10.3390/universe9020094

Hubble, E. (1929). A relation between distance and radial velocity among extra-galactic nebulae. *Proceedings of the National Academy of Sciences*, *15*(3), 168-173. https://doi.org/10.1073/pnas.15.3.168

Lemaître, G. (1927). Un Univers homogène de masse constante et de rayon croissant rendant compte de la vitesse radiale des nébuleuses extra-galactiques. *Annales de la Société Scientifique de Bruxelles*, *A47*, 49-59.

Lesgourgues, J. (2011). The Cosmic Linear Anisotropy Solving System (CLASS) I: Overview. *arXiv e-prints*. https://doi.org/10.48550/arXiv.1104.2932

Lesgourgues, J. (2023). *CLASS.* https://lesgourg.github.io/class_public/class.html (Accessed: 2023-11-22)

Lewis, A., & Challinor, A. (2023). *CAMB.* https://github.com/cmbant/camb (Accessed: 2023-10-17)

Lewis, A., Challinor, A., & Lasenby, A. (2000). Efficient Computation of Cosmic Microwave Background Anisotropies in Closed Friedmann-Robertson-Walker Models. *The Astrophysical Journal*, *538*(2), 473. https://doi.org/10.1086/309179

Li, Y.-H., & Zhang, X. (2023). IDECAMB: an implementation of interacting dark energy cosmology in CAMB. *arXiv e-prints*. https://doi.org/10.48550/arXiv.2306.01593

Majerotto, E., Sapone, D., & Amendola, L. (2004). Supernovae type Ia data favour coupled phantom energy. *arXiv e-prints*. https://doi.org/10.48550/arXiv.astro-ph/0410543

Massey, R., Rhodes, J., Ellis, R., Scoville, N., Leauthaud, A., Finoguenov, A., Capak, P., Bacon, D., Aussel, H., Kneib, J.-P., Koekemoer, A., McCracken, H., Mobasher, B., Pires, S., Refregier, A., Sasaki, S., Starck, J.-L., Taniguchi, Y., Taylor, A., & Taylor, J. (2007). Dark matter maps reveal cosmic scaffolding. *Nature*, *445*(7125), 286-290. https://doi.org/10.1038/nature05497

Mazde, K., & Visinelli, L. (2023). The interplay between the dark matter axion and primordial black holes. *Journal of Cosmology and Astroparticle Physics*, *2023*(01), 021. https://doi.org/10.1088/1475-7516/2023/01/021

Misiaszek, M., & Rossi, N. (2023). Direct detection of dark matter: a critical review. *arXiv e-prints*. https://doi.org/10.48550/arXiv.2310.20472

Misner, C. W., Thorne, K. S., & Wheeler, J. A. (1973). *Gravitation* (1st ed.). San Francisco: W. H. Freeman and Company.

Nesseris, S., Sapone, D., & Sypsas, S. (2020). Evaporating primordial black holes as varying dark energy. *Physics of the Dark Universe*, *27*, 100413. https://doi.org/10.1016/j.dark.2019.100413

Page, D. N. (1976). Particle emission rates from a black hole: Massless particles from an uncharged, nonrotating hole. *Physical Review D*, *13*, 198–206. https://doi.org/10.1103/PhysRevD.13.198

Peebles, P. J. E. (1993). *Principles of Physical Cosmology* (1st ed.). New Jersey: Princeton University Press.

Penzias, A. A., & Wilson, R. W. (1965). A Measurement of Excess Antenna Temperature at 4080 Mc/s. *The Astrophysical Journal*, *142*, 419-421. https://doi.org/10.1086/148307

Perlmutter, S., Aldering, G., Goldhaber, G., Knop, R. A., Nugent, P., Castro, P. G., Deustua, S., Fabbro, S., Goobar, A., Groom, D. E., Hook, I. M., Kim, A. G., Kim, M. Y., Lee, J. C., Nunes, N. J., Pain, R., Pennypacker, C. R., Quimby, R., Lidman, C., ... Project, T. S. C. (1999). Measurements of Ω and Λ from 42 High-Redshift Supernovae. *The Astrophysical Journal*, *517*(2), 565. https://doi.org/10.1086/307221

Planck Collaboration. (2020). *2018 CMB maps.* https://wiki.cosmos.esa.int/planck-legacy-archive/index.php/CMB_maps (Accessed: 2023-10-17)

Planck Collaboration, Ade, P. A. R., Aghanim, N., Arnaud, M., Ashdown, M., Aumont, J., Baccigalupi, C., Banday, A. J., Barreiro, R. B., Bartlett, J. G., Bartolo, N., Battaner,

E., Battye, R., Benabed, K., Benoît, A., Benoit-Lévy, A., Bernard, J.-P., Bersanelli, M., Bielewicz, P., ... Zonca, A. (2016). Planck 2015 results - XIII. Cosmological parameters. *Astronomy & Astrophysics*, *594*, A13. https://doi.org/10.1051/0004-6361/201525830

Planck Collaboration, Aghanim, N., Akrami, Y., Ashdown, M., Aumont, J., Baccigalupi, C., Ballardini, M., Banday, A. J., Barreiro, R. B., Bartolo, N., Basak, S., Benabed, K., Bernard, J.-P., Bersanelli, M., Bielewicz, P., Bock, J. J., Bond, J. R., Borrill, J., Bouchet, F. R., ... Zonca, A. (2020a). Planck 2018 results - V. CMB power spectra and likelihoods. *Astronomy & Astrophysics*, *641*, A5. https://doi.org/10.1051/0004-6361/201936386

Planck Collaboration, Aghanim, N., Akrami, Y., Ashdown, M., Aumont, J., Baccigalupi, C., Ballardini, M., Banday, A. J., Barreiro, R. B., Bartolo, N., Basak, S., Battye, R., Benabed, K., Bernard, J.-P., Bersanelli, M., Bielewicz, P., Bock, J. J., Bond, J. R., Borrill, J., ... Zonca, A. (2020b). Planck 2018 results - VI. Cosmological parameters. *Astronomy & Astrophysics*, *641*, A6. https://doi.org/10.1051/0004-6361/201833910

Planck Collaboration, Akrami, Y., Ashdown, M., Aumont, J., Baccigalupi, C., Ballardini, M., Banday, A. J., Barreiro, R. B., Bartolo, N., Basak, S., Benabed, K., Bersanelli, M., Bielewicz, P., Bond, J. R., Borrill, J., Bouchet, F. R., Boulanger, F., Bucher, M., Burigana, C., ... Zonca, A. (2020). Planck 2018 results - IV. Diffuse component separation. *Astronomy & Astrophysics*, *641*, A4. https://doi.org/10.1051/0004-6361/201833881

Riess, A. G., & Breuval, L. (2023). The Local Value of H_0. *arXiv e-prints*. https://doi.org/10.48550/arXiv.2308.10954

Riess, A. G., Filippenko, A. V., Challis, P., Clocchiatti, A., Diercks, A., Garnavich, P. M., Gilliland, R. L., Hogan, C. J., Jha, S., Kirshner, R. P., Leibundgut, B., Phillips, M. M., Reiss, D., Schmidt, B. P., Schommer, R. A., Smith, R. C., Spyromilio, J., Stubbs, C., Suntzeff, N. B., & Tonry, J. (1998). Observational evidence from supernovae for an accelerating universe and a cosmological constant. *The Astronomical Journal*, *116*(3), 1009. https://doi.org/10.1086/300499

Riess, A. G., Yuan, W., Macri, L. M., Scolnic, D., Brout, D., Casertano, S., Jones, D. O., Murakami, Y., Anand, G. S., Breuval, L., Brink, T. G., Filippenko, A. V., Hoffmann, S., Jha, S. W., Kenworthy, W. D., Mackenty, J., Stahl, B. E., & Zheng, W. (2022). A Comprehensive Measurement of the Local Value of the Hubble Constant with $1\,\mathrm{km\,s^{-1}\,Mpc^{-1}}$ Uncertainty from the Hubble Space Telescope and the SH0ES Team. *The Astrophysical Journal Letters*, *934*(1), L7. https://doi.org/10.3847/2041-8213/ac5c5b

Roszkowski, L., Sessolo, E. M., & Trojanowski, S. (2018). WIMP dark matter candidates and searches—current status and future prospects. *Reports on Progress in Physics*, *81*(6), 066201. https://doi.org/10.1088/1361-6633/aab913

Rubin, V. C., & Ford, J., W. Kent. (1970). Rotation of the Andromeda Nebula from a Spectroscopic Survey of Emission Regions. *The Astrophysical Journal*, *159*, 379. https://doi.org/10.1086/150317

Ryden, B. (2006). *Introduction to Cosmology*. Ohio: Department of Astronomy, The Ohio State Univeristy.

Sapone, D. (2023, October 18). *Lecture notes in cosmology* [Lecture presentation].

Schwarzschild, K. (1916). On the gravitational field of a mass point according to Einstein's

theory. *Sitzungsber. Preuss. Akad. Wiss. Berlin (Math.Phys.)*, 189-196. https://doi.org/10.48550/arXiv.physics/9905030

Slipher, V. M. (1915). Spectrographic Observations of Nebulae. *Popular Astronomy*, *23*, 21-24.

Stokes, G. G. (2009). On the Composition and Resolution of Streams of Polarized Light from different Sources. In *Mathematical and physical papers* (Vol. 3, p. 233–258). Cambridge University Press. https://doi.org/10.1017/CBO9780511702266.010

The Event Horizon Telescope Collaboration, Akiyama, K., Alberdi, A., Alef, W., Asada, K., Azulay, R., Baczko, A.-K., Ball, D., Baloković, M., Barrett, J., Bintley, D., Blackburn, L., Boland, W., Bouman, K. L., Bower, G. C., Bremer, M., Brinkerink, C. D., Brissenden, R., Britzen, S., ... Ziurys, L. (2019). First M87 Event Horizon Telescope Results. I. The Shadow of the Supermassive Black Hole. *The Astrophysical Journal Letters*, *875*(1), L1. https://doi.org/10.3847/2041-8213/ab0ec7

Torrado, J., & Lewis, A. (2019). *Cobaya: Bayesian analysis in cosmology.* Astrophysics Source Code Library, record ascl:1910.019. https://ascl.net/1910.019

Torrado, J., & Lewis, A. (2021). Cobaya: code for Bayesian analysis of hierarchical physical models. *Journal of Cosmology and Astroparticle Physics*, *2021*(05), 057. https://doi.org/10.1088/1475-7516/2021/05/057

Verde, L. (2007). A practical guide to Basic Statistical Techniques for Data Analysis in Cosmology. *arXiv e-prints*. https://doi.org/10.48550/arXiv.0712.3028

Wald, R. M. (1984). *General Relativity* (1st ed.). Chicago & London: The University of Chicago Press.

Weinberg, S. (1978). A New Light Boson? *Physical Review Letters*, *40*, 223–226. https://doi.org/10.1103/PhysRevLett.40.223

Weinberg, S. (2008). *Cosmology* (1st ed.). New York: Oxford University Press Inc.

Zel'dovich, Y. B., & Novikov, I. D. (1967). The Hypothesis of Cores Retarded during Expansion and the Hot Cosmological Model. *Astronomicheskii Zhurnal*, *43*, 758. https://ui.adsabs.harvard.edu/abs/1966AZh....43..758Z

Zwicky, F. (1933). Die Rotverschiebung von extragalaktischen Nebeln. *Helvetica Physica Acta*, *6*, 110-127.

ANNEXES

Annex A

`CLASS` code detailed modification

`CLASS` code version 3.2.1 was adapted to the PBH model by modifying both C and Python files as follows

1. Modifications in C files

   (a) *tools/evolver_pbhs.c*: Only the *evolver_pbhs.c* file located in the *tools* folder was created. It is a copy of *evolver_ndf15.c*, it has the same functions, but with different names (adding "_pbhs" at the end of each) and allows PBHs to evaporate completely, by modifying

```
465:     else if (absh <= hmin){
466:       // Added by JPBU
467:       abshlast = absh;
468:       absh = MAX(0.3 * absh, hmin);
469:       h = tdir * absh;
470:       done = _FALSE_;
471:       adjust_stepsize_pbhs(dif,(absh/abshlast),neq,k);
472:       hinvGak = h * invGa[k-1];
473:       nconhk = 0;
474:       break;
475:       //class_test(absh <= hmin, error_message,
476:       //           ''Step size too small: step:%g,
                      minimum:%g, in interval: [%g:%g]\n'',
477:       //           absh,hmin,t0,tfinal);
478:     }

502:     if (err>rtol){
503:       /*Step failed */
504:       stepstat[1]+= 1;
505:       if (absh <= hmin){
506:         // Added by JPBU
```

```
507:          nofailed = _FALSE_;
508:          hopt = absh * MAX(0.1, 0.833*pow((rtol/err),
              (1.0/(k+1))));
509:          if (k > 1){
510:            errkm1 = 0.0;
511:            for(jj=1;jj<=neq;jj++){
512:              errkm1 = MAX(errkm1,fabs((dif[jj][k]
                  +difkp1[jj])*invwt[jj]));
513:            }
514:            errkm1 = errkm1*erconst[k-2];
515:            hkm1 = absh * MAX(0.1, 0.769*pow((rtol
                  /errkm1),(1.0/k)));
516:            if (hkm1 > hopt){
517:              hopt = MIN(absh,hkm1);
                  /* don't allow step size increase */
518:              k = k - 1;
519:            }
520:          }
521:          absh = MAX(hmin, hopt);
522:          break;
523:          //class_test(absh <= hmin, error_message,
524:          //             ''Step size too small: step:%g,
                           minimum:%g, in interval: [%g:%g]\n'',
525:          //             absh,hmin,t0,tfinal);
526:        }
```

(b) *source*: The *input.c* and *background.c* files located in the *source* folder were modified as follows

i. *input.c*

```
3355:     /* Evaporating PBH model (added by JPBU) */
3356:     /** 8.c) Additional PBH parameters */
3357:     /* Read */
3358:     class_read_double(''f_PBH'',pba->f_PBH);
3359:     class_read_double(''alpha_PBH'',pba->alpha_PBH);
3360:     class_read_double(''w_x'',pba->w_x);
3361:     /* Evaporating PBH model */

5824:     /* Evaporating PBH model (added by JPBU) */
5825:     pba->f_PBH = 0.;
5826:     /* Evaporating PBH model */

5851:     /** 9.c) PBH (added by JPBU) */
5852:     pba->alpha_PBH = -10.;
5853:     pba->w_x = 1./3.;
```

Parameters $f_{\rm PBH}$ (written as f_PBH), $\log(\tilde{\alpha})$[28] (alpha_PBH) and w_X (w_x)

[28]Here, $\log(\tilde{\alpha})$ means $\log_{10}(\tilde{\alpha})$ and is preferable to using $\tilde{\alpha}$ to avoid code stability problems.

were defined in the file *input.c*, assuming $f_{\rm PBH} = 0$, $\log(\tilde{\alpha}) = -10$ and $w_X = 1/3$ if the user does not set their values.

ii. *background.c*

```
371:    /* Evaporating PBH model (added by JPBU) */
372:    double astar, Ostar_x;     // global variables
373:    /* Evaporating PBH model (added by JPBU) */

401:    /* Hubble's parameter (added by JPBU) */
402:    double H;

407:    /* Evaporating PBH model (added by JPBU) */
408:    double O_PBH, O_x;
409:    /* Evaporating PBH model */

446:    /* cdm (modified by JPBU) */
447:    if (pba->has_cdm == _TRUE_
        && pba->has_PBH == _FALSE_) {

454:    /* Evaporating PBH model (added by JPBU) */
455:    if (pba->has_cdm == _TRUE_
        && pba->has_PBH == _TRUE_) {
456:      pvecback[pba->index_bg_rho_cdm] = (1.
          -pba->f_PBH)*pba->Omega0_cdm
          * pow(pba->H0,2) / pow(a,3);
457:      rho_tot += pvecback[pba->index_bg_rho_cdm];
458:      p_tot += 0.;
459:      rho_m += pvecback[pba->index_bg_rho_cdm];
460:    }
461:    /* Evaporating PBH model */

510:    /* Evaporating PBH model (added by JPBU) */
511:    if (pba->has_PBH == _TRUE_){

513:      O_PBH = pvecback_B[pba->index_bi_O_PBH];
          // \tilde{\Omega_{PBH}}
514:      O_x   = pvecback_B[pba->index_bi_O_x];
          // \tilde{\Omega_{x}}

516:      // Added by JPBU
517:      pvecback[pba->index_bg_astar] = 0;
          // a when \tilde{\Omega_{PBH}} = 0
518:      pvecback[pba->index_bg_Ostar_x] = 0;
          // \tilde{\Omega_{x}} when
          \tilde{\Omega_{PBH}} = 0

520:      if (O_PBH < 0) {
```

```
521:          O_PBH = 0;
522:          O_x = Ostar_x * pow(astar,3.*(1.+pba->w_x))
              / pow(pba->H0,2);
523:        }

525:        pvecback[pba->index_bg_rho_PBH] = O_PBH
            * pow(pba->H0,2) / pow(a,3); // \rho_{PBH}
526:        rho_tot += pvecback[pba->index_bg_rho_PBH];
527:        pvecback[pba->index_bg_rho_x]    = O_x
            * pow(pba->H0,2) / pow(a,3.*(1.+pba->w_x));
            // \rho_{x}
528:        rho_tot += pvecback[pba->index_bg_rho_x];

530:        if (O_PBH < 3.e-9 && O_PBH > 0) {
531:          astar = a;
532:          Ostar_x = pvecback[pba->index_bg_rho_x];
533:          pvecback[pba->index_bg_astar] = astar;
534:          pvecback[pba->index_bg_Ostar_x] = Ostar_x;
535:        }

537:        /** Pressure in evaporating PBH model */

539:        /* P_{PBH} = 0 */
540:        pvecback[pba->index_bg_p_x]    = pba->w_x
            *pvecback[pba->index_bg_rho_x];
541:        p_tot += pvecback[pba->index_bg_p_x];
542:        dp_dloga += 0.0;

544:        rho_m += pvecback[pba->index_bg_rho_PBH];
            // PBHs contributes matter?
545:        rho_r += pvecback[pba->index_bg_rho_x];
            // Dark radiation contributes radiation?
546:      }
547:      /* Evaporating PBH model */

636:      H = sqrt(rho_tot-pba->K/a/a); /* PBH: Short
          notations for use in the following equations
          (added by JPBU) */

639:      /* Evaporating PBH model (added by JPBU) */
640:      /*  Add P_PBH_prime here */
641:      if (pba->has_PBH == _TRUE_) {
642:        pvecback[pba->index_bg_O_PBH] = pvecback[pba
          ->index_bg_rho_PBH] / pow(H,2);
643:        pvecback[pba->index_bg_O_x]    = pvecback[pba
          ->index_bg_rho_x] / pow(H,2);
644:        /* P_{PBH}' = 0 */
```

```
646:        /* P_{x}' */
647:        dp_dloga += -3.*(1.+pba->w_x)*pba->w_x
            *pvecback[pba->index_bg_rho_x]
            + (pow(10,pba->alpha_PBH)*pba->w_x
            *pow(H,5.)*pow(pba->f_PBH
            *pba->Omega0_cdm,3))/(pow(a,9)*H
            *pow(pvecback[pba->index_bg_rho_PBH],2))
            + 2*pvecback[pba->index_bg_rho_PBH];
648:      }
649:      /* Evaporating PBH model */

1050:     /* Evaporating PBH model (added by JPBU) */
1051:     pba->has_PBH = _FALSE_;
1052:     /* Evaporating PBH model */

1078:     /* Evaporating PBH model (added by JPBU) */
1079:     if (pba->f_PBH != 0.)
1080:     pba->has_PBH = _TRUE_;
1081:     /* Evaporating PBH model */

1150:     /* Evaporating PBH model (added by JPBU) */
1151:     /* - indices for PBH */
1152:     class_define_index(pba->index_bg_astar,
          pba->has_PBH,index_bg,1);
1153:     class_define_index(pba->index_bg_Ostar_x,
          pba->has_PBH,index_bg,1);
1154:     class_define_index(pba->index_bg_O_PBH,
          pba->has_PBH,index_bg,1);
1155:     class_define_index(pba->index_bg_O_x,
          pba->has_PBH,index_bg,1);
1156:     class_define_index(pba->index_bg_rho_PBH,
          pba->has_PBH,index_bg,1);
1157:     class_define_index(pba->index_bg_rho_x,
          pba->has_PBH,index_bg,1);
1158:     class_define_index(pba->index_bg_p_x,
          pba->has_PBH,index_bg,1);
1159:     /* Evaporating PBH model */

1257:     /* Evaporating PBH model (added by JPBU) */
1258:     /* -> PBH and its derivative wrt a */
1259:     class_define_index(pba->index_bi_O_PBH,
          pba->has_PBH,index_bi,1);
1260:     class_define_index(pba->index_bi_O_x,
          pba->has_PBH,index_bi,1);
1261:     /* Evaporating PBH model */
```

```
1986:     /* Evaporating PBH model (added by JPBU) */
1987:     extern int evolver_pbhs();
1988:     /* Evaporating PBH model (added by JPBU) */

2057:     /* Evaporating PBH model (added by JPBU) */
2058:     if (pba->has_PBH == _TRUE_) {
2059:       generic_evolver = evolver_pbhs;
2060:     }
2061:     /* Evaporating PBH model (added by JPBU) */

2191:     /* Evaporating PBH model (added by JPBU) */
2192:     if (pba->has_PBH == _TRUE_) {
2193:       printf(``     Primodial Black Hole:\n'');
2194:       printf(``      -> Omega0_PBH = %g, and
          Omega0_x %g\n'',
2195:              pba->background_table[(pba->bt_size-1)
               *pba->bg_size+pba->index_bg_rho_PBH]
               /pba->background_table[(pba->bt_size-1)
               *pba->bg_size+pba->index_bg_rho_crit],
               pba->background_table[(pba->bt_size-1)
               *pba->bg_size+pba->index_bg_rho_x]
               /pba->background_table[(pba->bt_size-1)
               *pba->bg_size+pba->index_bg_rho_crit]);

2197:       printf(``f_PBH -> %.g \n'',pba->f_PBH);
2198:       printf(``alpha -> %.g \n'',pow(10,
          pba->alpha_PBH));
2199:       printf(``w_x   -> %.g \n'',pba->w_x);
2200:     }
2201:     /* Evaporating PBH model */

2407:     /* Evaporating PBH model (added by JPBU) */
2408:     // Fix initial value of \tilde{\Omega}_{PBH}
2409:     if (pba->has_PBH == _TRUE_) {
2410:     pvecback_integration[pba->index_bi_O_PBH] =
          pba->f_PBH*pba->Omega0_cdm;
2411:     pvecback_integration[pba->index_bi_O_x] = 0.;

2413:     // test
2414:     class_test(!isfinite(pvecback_integration[pba
          ->index_bi_O_PBH]) ||
2415:                !isfinite(pvecback_integration[pba
                   ->index_bi_O_PBH]),
2416:                pba->error_message,
2417:                ``initial Omega_PBH_ini = %e
                   -> check initial conditions'',
2418:                pvecback_integration[pba
```

```
                    ->index_bi_O_PBH]);

2420:     class_test(!isfinite(pvecback_integration[pba
          ->index_bi_O_x]) ||
2421:                !isfinite(pvecback_integration[pba
                    ->index_bi_O_x]),
2422:                pba->error_message,
2423:                ``initial Omega_x_ini = %e
                    -> check initial conditions'',
2424:                pvecback_integration[pba
                    ->index_bi_O_x]);
2425:     }
2426:     /* Evaporating PBH model */

2603:     /* Evaporating PBH model (added by JPBU) */
2604:     class_store_columntitle(titles,``(.)astar'',
          pba->has_PBH);
2605:     class_store_columntitle(titles,``(.)Omegastar_x'',
          pba->has_PBH);
2606:     class_store_columntitle(titles,``(.)Omega_PBH'',
          pba->has_PBH);
2607:     class_store_columntitle(titles,``(.)Omega_x'',
          pba->has_PBH);
2608:     class_store_columntitle(titles,``(.)rho_PBH'',
          pba->has_PBH);
2609:     class_store_columntitle(titles,``(.)rho_x'',
          pba->has_PBH);
2610:     class_store_columntitle(titles,``(.)p_x'',
          pba->has_PBH);
2611:     /* Evaporating PBH model */

2686:     /* Evaporating PBH model (added by JPBU) */
2687:     class_store_double(dataptr,pvecback[pba
          ->index_bg_astar],pba->has_PBH,storeidx);
2688:     class_store_double(dataptr,pvecback[pba
          ->index_bg_Ostar_x],pba->has_PBH,storeidx);
2689:     class_store_double(dataptr,pvecback[pba
          ->index_bg_O_PBH],pba->has_PBH,storeidx);
2690:     class_store_double(dataptr,pvecback[pba
          ->index_bg_O_x],pba->has_PBH,storeidx);
2691:     class_store_double(dataptr,pvecback[pba
          ->index_bg_rho_PBH],pba->has_PBH,storeidx);
2692:     class_store_double(dataptr,pvecback[pba
          ->index_bg_rho_x],pba->has_PBH,storeidx);
2693:     class_store_double(dataptr,pvecback[pba
          ->index_bg_p_x],pba->has_PBH,storeidx);
2694:     /* Evaporating PBH model */
```

```
2817:     /* Evaporating PBH model (added by JPBU) */
2818:     if (pba->has_PBH == _TRUE_) {
2819:       dy[pba->index_bi_O_PBH] = -pow(10,pba
          ->alpha_PBH)*pba->H0*pow(pba->f_PBH
          *pba->Omega0_cdm,3)/pow(y[pba
          ->index_bi_O_PBH],2)/H;
2820:       dy[pba->index_bi_O_x] = pow(10,pba
          ->alpha_PBH)*pba->H0*pow(a,3.*pba->w_x)
          *pow(pba->f_PBH*pba->Omega0_cdm,3)/pow(y[pba
          ->index_bi_O_PBH],2)/H;
2821:     }
2822:     /* Evaporating PBH model */

3031:     /* Evaporating PBH model (added by JPBU) */
3032:     if (pba->has_PBH == _TRUE_) {
3033:       printf(" Primordial Black Hole
          f_PBH = %-15g , alpha = %-15g\n",pba->f_PBH,
          pow(10,pba->alpha_PBH));
3034:     }
3035:     /* Evaporating PBH model */
```

a^* (astar) and $\tilde{\Omega}_X^*$ (Ostar_x) are defined in the *background.c* file as global variables consisting of the scale factor and $\tilde{\Omega}_X$ when $\tilde{\Omega}_{\rm PBH} = 0$, respectively (see lines 372 and 530-535). The Hubble parameter H (H) is defined as $\sqrt{\rho_{\rm tot} - K/a^2}$ for use on lines 642, 643 and 647. Also, $\tilde{\Omega}_{\rm PBH}$ (O_PBH) and $\tilde{\Omega}_X$ (O_x) are introduced in this file (see lines 408, 513 and 514). If $\tilde{\Omega}_{\rm PBH} < 0$, PBHs have already evaporated, so it is necessary to assume $\tilde{\Omega}_{\rm PBH} = 0$ and $\tilde{\Omega}_{\rm PBH} = \tilde{\Omega}_X^* a^{*3(1+w_X)}$ (see lines 520-523). Since `CLASS` works with the real[29] density ρ, $\rho_{\rm PBH}$ (pvecback[pba→index_bg_rho_PBH]) and ρ_X (pvecback[pba→index_bg_rho_x]) are defined as $\rho_{\rm PBH} = \tilde{\Omega}_{\rm PBH} H_0^2/a^3$ and $\rho_X = \tilde{\Omega}_X H_0^2/a^{3(1+w_X)}$, taking (2.19) into account (see lines 525 and 527). The evolver _pbhs function, defined in tools/evolver_pbhs.c, is used to solve the differential equations for PBHs (see the system of equations (5.1) and the lines 1987, 2058-2060 and 2818-2821), with $\tilde{\Omega}_{\rm PBH}(a_{\rm in}) = f_{\rm PBH}\Omega_{c,0}$ and $\tilde{\Omega}_X(a_{\rm in}) = 0$ as initial conditions (see lines 2409-2425), where $a_{\rm in} = 10^{-14}$ is the initial time defined in `CLASS`.

(c) *include*: The *evolver_pbhs.h* and *background.h* files located in the *include* folder were created and modified, respectively, as follows

i. *evolver_pbhs.h*
This archive is a copy of *evolver_ndf15.h*; it only changed the name of the functions (adding "_pbhs" at the end of each).

ii. *background.h*

```
125:     /* Evaporating PBH model (added by JPBU) */
126:     double f_PBH;       /**< Fraction of dark*/
```

[29] In the sense that has density units (instead, Ω is adimensional).

```
                                /**< energy in form of PBH */
127:    double alpha_PBH;       /**< parameter related to*/
                                /**< the initial mass of BH */
128:    double w_x;             /**< eqn of state of DR */
129:    /* Evaporating PBH model */

194:    /* Evaporating PBH model (added by JPBU) */
195:    int index_bg_astar;
        /**< a when \tilde{\Omega}_{PBH} = 0 */
196:    int index_bg_Ostar_x; /**< \tilde{\Omega}_{x}
        when \tilde{\Omega}_{PBH} = 0 */
197:    int index_bg_O_PBH;     /**< tilde{Omega}_{PBH}*/
198:    int index_bg_O_x;       /**< tilde{Omega}_{X} */
199:    int index_bg_rho_PBH; /**< PBH energy density */
200:    int index_bg_rho_x;     /**< DR energy density */
201:    int index_bg_p_x;       /**< DR pressure */
202:    /* Evaporating PBH model */

280:    /* Evaporating PBH model (added by JPBU) */
281:    int index_bi_O_PBH; /**< {B} PBH value*/
                            /**< $tilde{Omega}_{PBH}$ */
282:    int index_bi_O_x;   /**< {B}    DR value*/
                            /**< $tilde{Omega}_{X}$ */
283:    /* Evaporating PBH model */

311:    /* Evaporating PBH model (added by JPBU) */
312:    short has_PBH;          /**< presence of a PBH? */
313:    /* Evaporating PBH model */
```

Parameters $f_{\rm PBH}$ (f_PBH), $\log(\tilde{\alpha})$ (alpha_PBH) and w_X (w_x), indexes associated with a^* (index_bg_astar), $\tilde{\Omega}^*_X$ (index_bg_Ostar_x), $\tilde{\Omega}_{\rm PBH}$ (index_bg_O_PBH and index_bi_O_PBH), $\tilde{\Omega}_X$ (index_bg_O_x and index_bi_O _x), $\rho_{\rm PBH}$ (index_bg_rho_PBH), ρ_X (index_bg_O_PBH) and dark radiation pressure p_X (index_bg_p_x), and a Boolean if PBH model is considered (has_PBH) is introduced in the *background.h* header file.

2. Modifications in Python files: The *cclassy.pxd* and *classy.pyx* files located in the *python* folder were modified as follows

   (a) *cclassy.pxd*

```
94:     ### Evaporating PBHs model (added by JPBU) ###
95:     double f_PBH
96:     double alpha_PBH
97:     double w_x
98:     ### Evaporating PBHs model ###
```

   Parameters $f_{\rm PBH}$ (f_PBH), $\log(\tilde{\alpha})$ (alpha_PBH) and w_X (w_x) are introduced in the *cclassy.pxd* file.

(b) *classy.pyx*

```
2473:        ### Evaporating PBHs model (added by JPBU) ###
2474:        elif name == 'f_PBH':
2475:              value = self.ba.f_PBH
2476:        elif name == 'alpha_PBH':
2477:              value = self.ba.alpha_PBH
2478:        elif name == 'w_x':
2479:              value = self.ba.w_x
2480:        ### Evaporating PBHs model ###
```

Parameters $f_{\rm PBH}$ (f_PBH), $\log(\tilde{\alpha})$ (alpha_PBH) and w_X (w_x) are introduced in the *classy.pyx* file, linking them with the definitions made in the C files.

After modifying `CLASS` files, it is necessary to do `make clean` and `make` in the terminal inside the *class* folder to compile it and `python setup.py build` and `python setup.py install --user` in the terminal inside the *python* folder to use `CLASS` with Python (it is also mandatory to restart the Python kernel if it is already running)[30].

[30]Here, `user` means literally `user` and not the name of the computer's user.

Annex B

Stokes parameters and polarization

The Stokes parameters (I, Q, U and V), defined by Stokes (2009) in 1852, describe the polarization state of electromagnetic radiation as follows

$$I = \langle E_1 E_1^* + E_2 E_2^* \rangle = A_1^2 + A_2^2 \tag{6.1}$$
$$Q = \langle E_1 E_1^* - E_2 E_2^* \rangle = A_1^2 - A_2^2 \tag{6.2}$$
$$U = \langle E_1 E_2^* + E_2 E_1^* \rangle = 2A_1 A_2 \cos(\phi_2 - \phi_1) \tag{6.3}$$
$$V = -i\langle E_1 E_2^* - E_2 E_1^* \rangle = 2A_1 A_2 \sin(\phi_2 - \phi_1), \tag{6.4}$$

where it has been considered a plane wave solution for the electric field $\mathbf{E}(t,z) = E_1(t,z)\hat{\epsilon}_\mathbf{1} + E_2(t,z)\hat{\epsilon}_\mathbf{2}$, with $E_1(t,z) = A_1 e^{i\phi_1} e^{i(kz-\omega t)}$ and $E_2(t,z) = A_2 e^{i\phi_2} e^{i(kz-\omega t)}$, A_j and ϕ_j the amplitude and the phase of the wave (with $j \in \{1,2\}$), respectively, k the wave number and ω its angular frequency.

Because the polarization of CMB photons is linear, $V = 0$ (V is nonzero only for circular polarization) and E and B modes correspond to the orientation in polarization Q and its change in amplitude U in the basis of the Fourier wave vector for small sections of the sky (Dodelson, 2003; Sapone, 2023).

Annex C

CLASS test

The CLASS code is tested in the background considering as a base the best-fit cosmological parameter values of Planck Collaboration, Aghanim, N., et al. (2020b), that is $H_0 = 67.32\,\mathrm{km\,s^{-1}\,Mpc^{-1}}$, $\Omega_{b,0}h^2 = 0.022\,377$, $\Omega_{c,0}h^2 = 0.120\,10$, $n_s = 0.9659$ and $\ln(10^{10}A_s) = 3.0447$, where $h = H_0/100$ is the reduced Hubble constant, n_s is scalar spectrum power-law index and A_s is the power of the primordial curvature perturbations[31].

In the first place, it is tested without considering the PBH model, to see if it works properly, plotting the densities background evolution illustrated in the Figure 6.1.

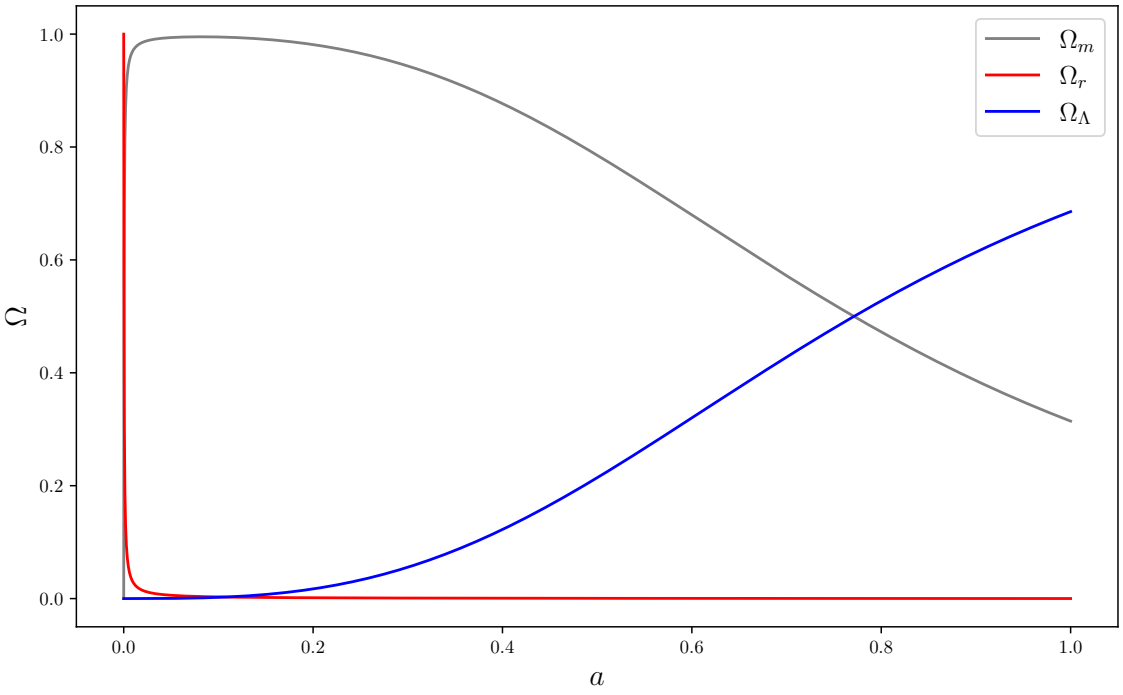

Figure 6.1: Densities background evolution considering ΛCDM.

[31]This values can be found in the **base_plikHM_TTTEEE_lowl_lowE** table, which is in https://wiki.cosmos.esa.int/planck-legacy-archive/images/4/43/Baseline_params_table_2018_68pc_v2.pdf.

In the second place, the code is tested considering that all dark matter consist of PBHs (that is, $f_{\mathrm{PBH}} = 1$) and the densities background evolution are plotted for different initial masses of PBHs (in the asteroidal to sublunar mass region), being illustrated in the Figures 6.2, 6.3, 6.4 for $M_{\mathrm{in}} \sim 10^{17}\,\mathrm{g}$, and 6.5, 6.6, 6.7 for $M_{\mathrm{in}} \sim 10^{22}\,\mathrm{g}$.

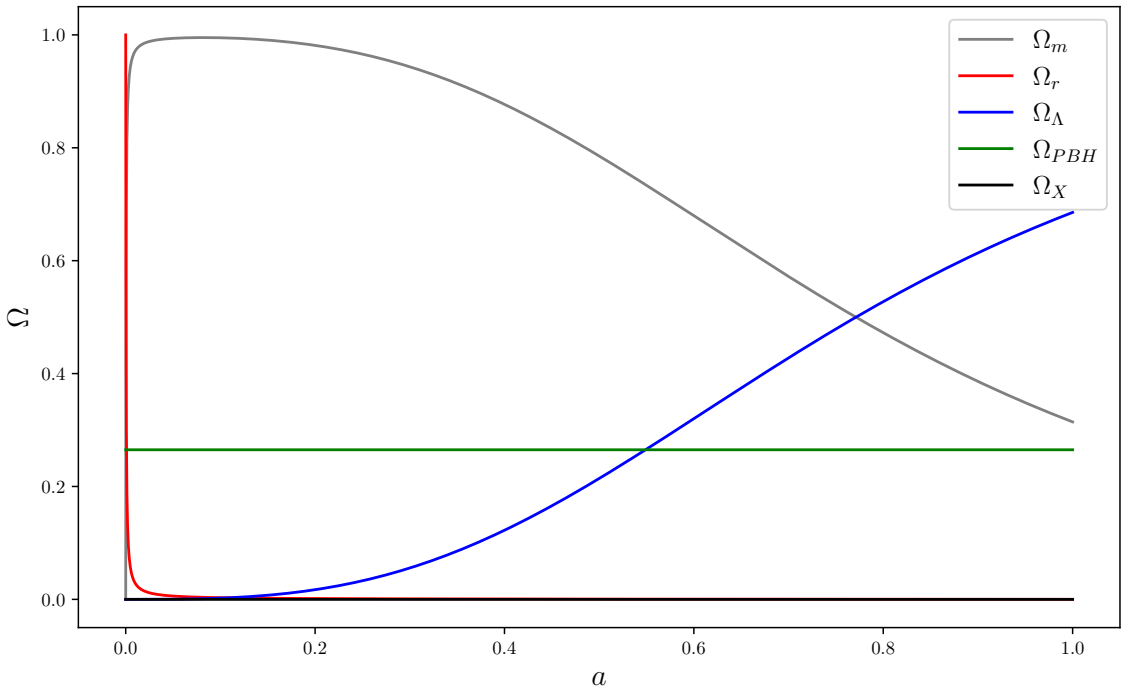

Figure 6.2: Densities background evolution considering $f_{\mathrm{PBH}} = 1$ and $M_{\mathrm{in}} \sim 10^{17}\,\mathrm{g}$.

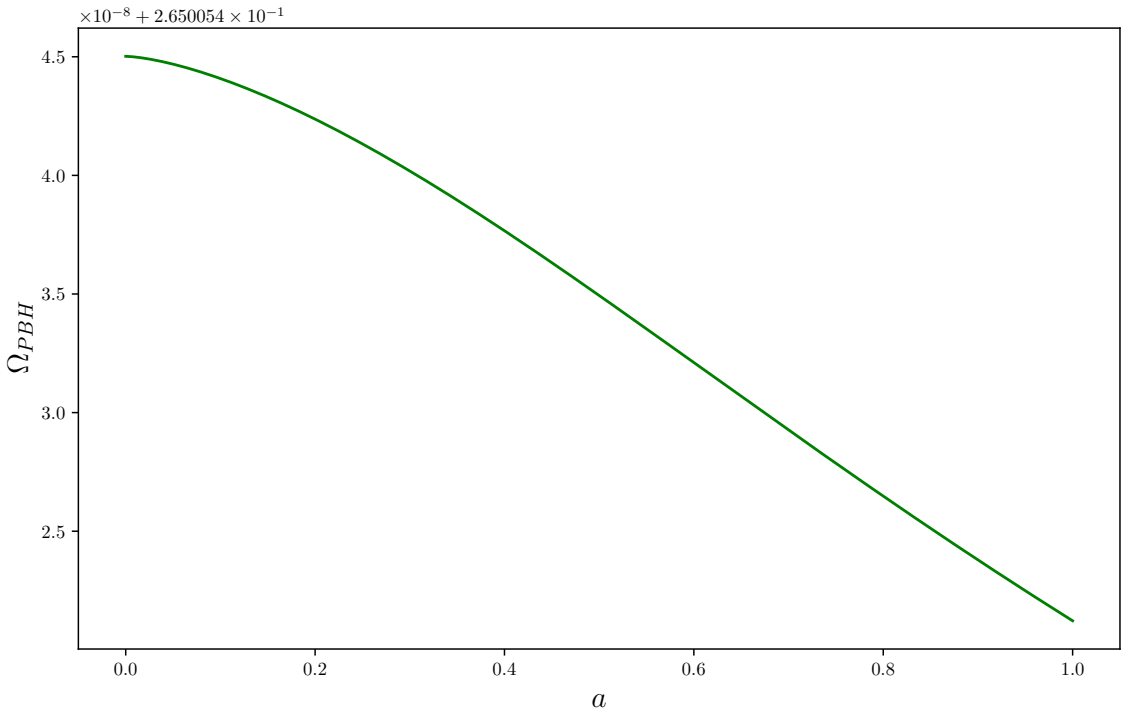

Figure 6.3: Ω_{PBH} background evolution considering $f_{\mathrm{PBH}} = 1$ and $M_{\mathrm{in}} \sim 10^{17}\,\mathrm{g}$.

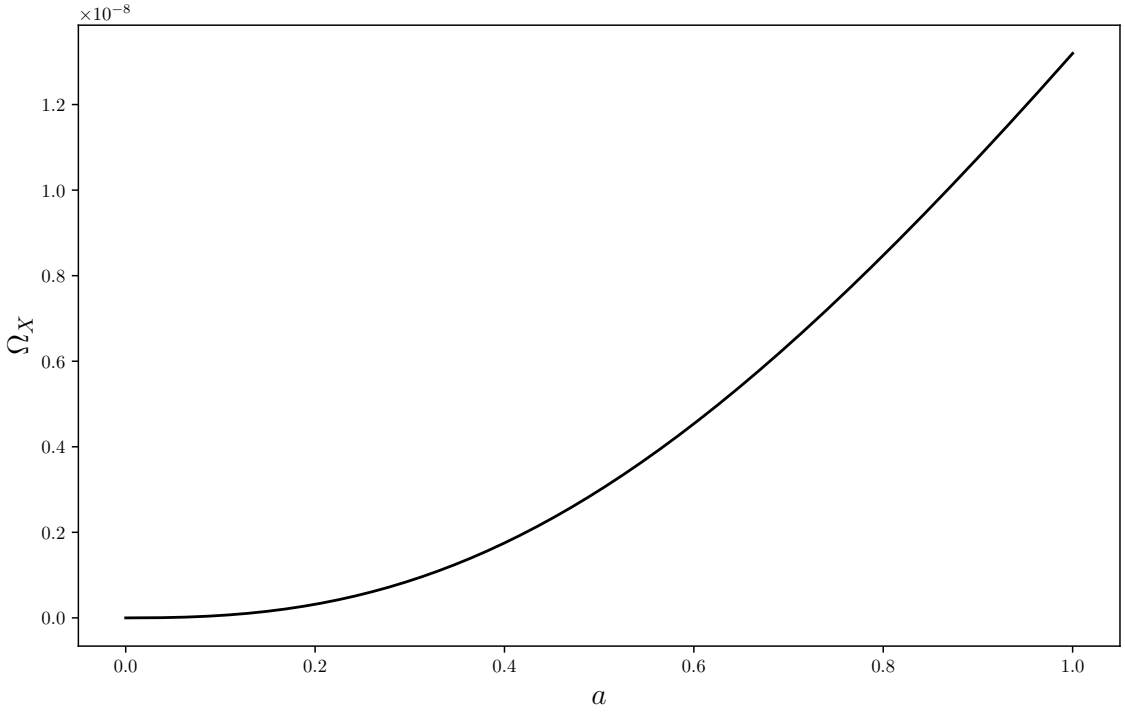

Figure 6.4: Ω_X background evolution considering $f_{\mathrm{PBH}} = 1$ and $M_{\mathrm{in}} \sim 10^{17}\,\mathrm{g}$.

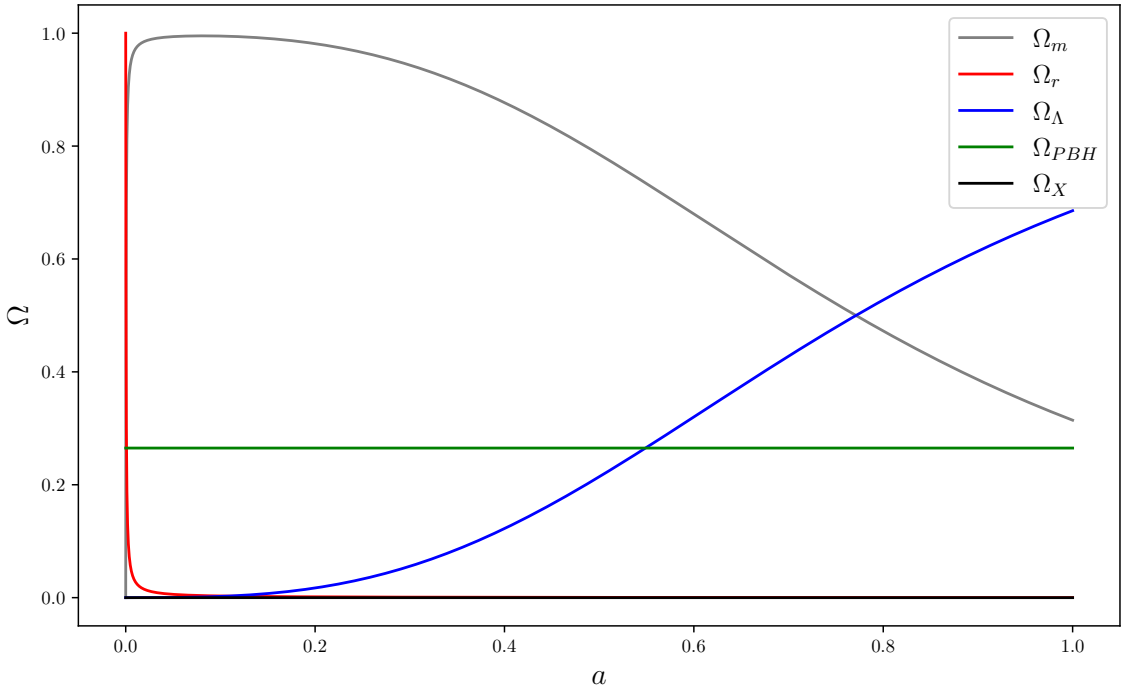

Figure 6.5: Densities background evolution considering $f_{\mathrm{PBH}} = 1$ and $M_{\mathrm{in}} \sim 10^{22}\,\mathrm{g}$.

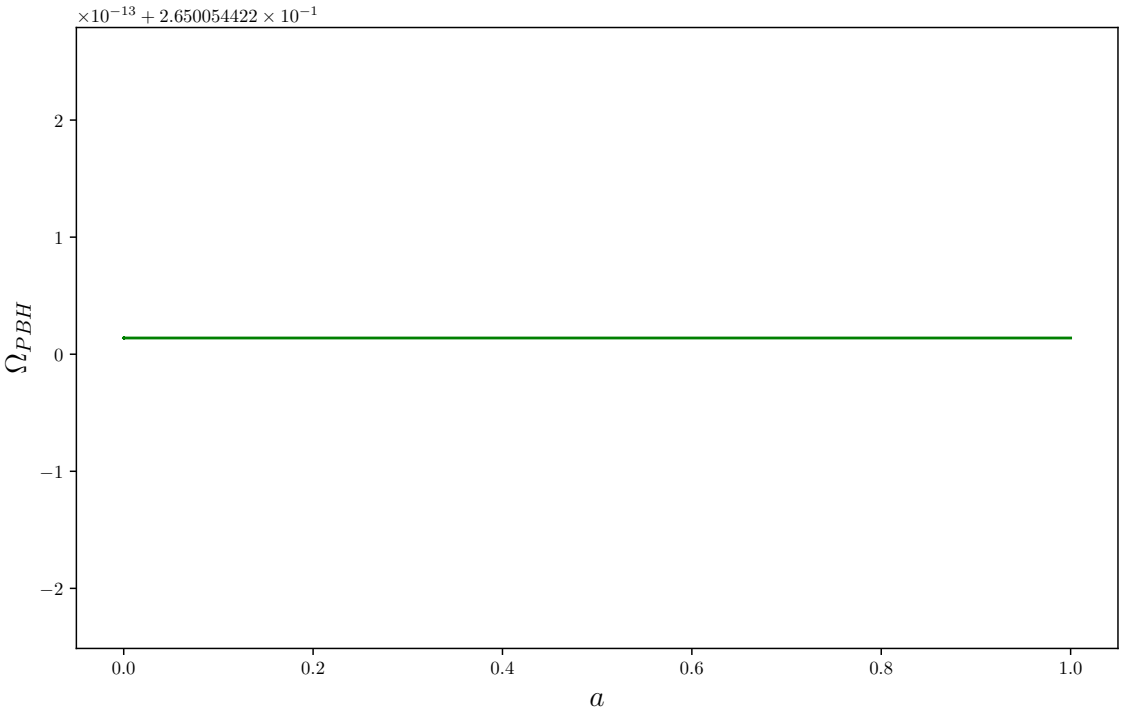

Figure 6.6: $\Omega_{\rm PBH}$ background evolution considering $f_{\rm PBH} = 1$ and $M_{\rm in} \sim 10^{22}\,{\rm g}$.

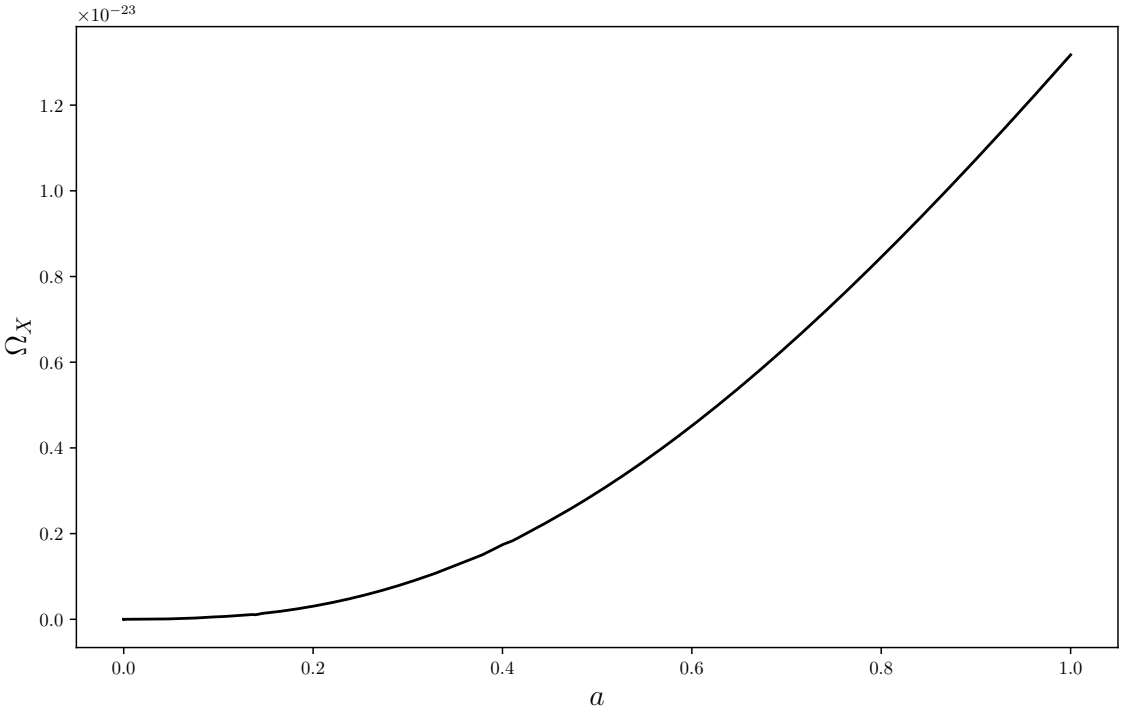

Figure 6.7: Ω_X background evolution considering $f_{\rm PBH} = 1$ and $M_{\rm in} \sim 10^{22}\,{\rm g}$.

In the third place, `CLASS` is tested searching for the lowest possible initial masses of PBHs before complete evaporation. It is found that the lowest initial mass is $M_{\rm in} = 6.46 \times 10^{14}\,\mathrm{g}$ (see Figures 6.8 and 6.9, where it is considered $f_{\rm PBH} = 10^{-7}$).

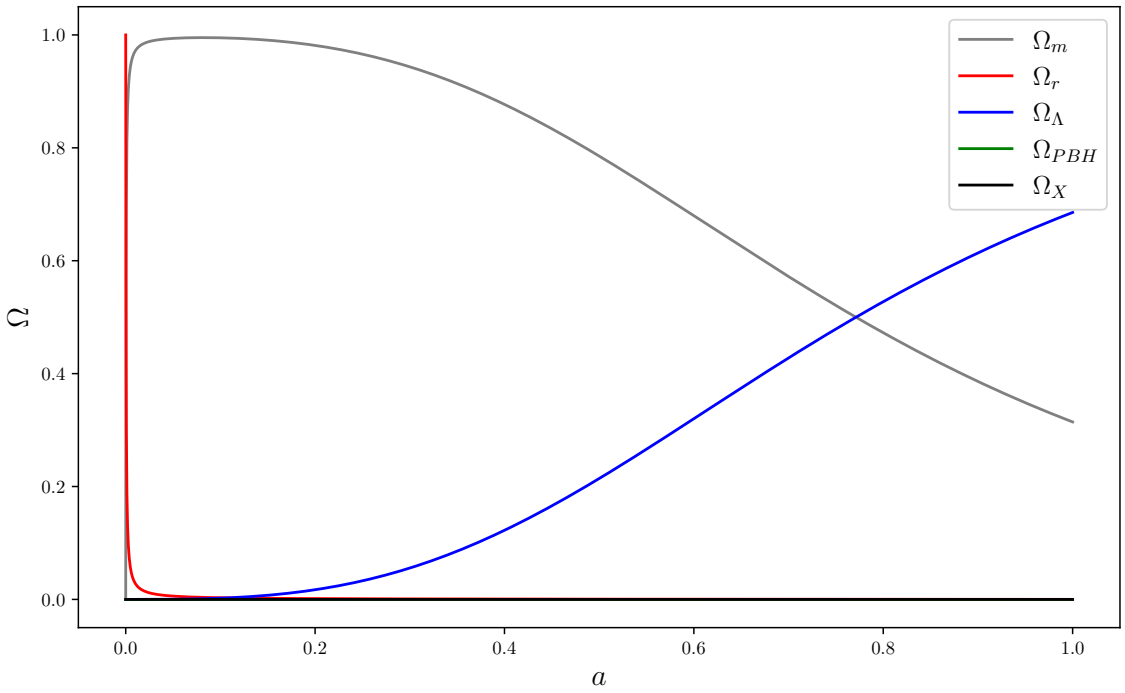

Figure 6.8: Densities background evolution considering $f_{\rm PBH} = 10^{-7}$ and $M_{\rm in} = 6.46 \times 10^{14}\,\mathrm{g}$.

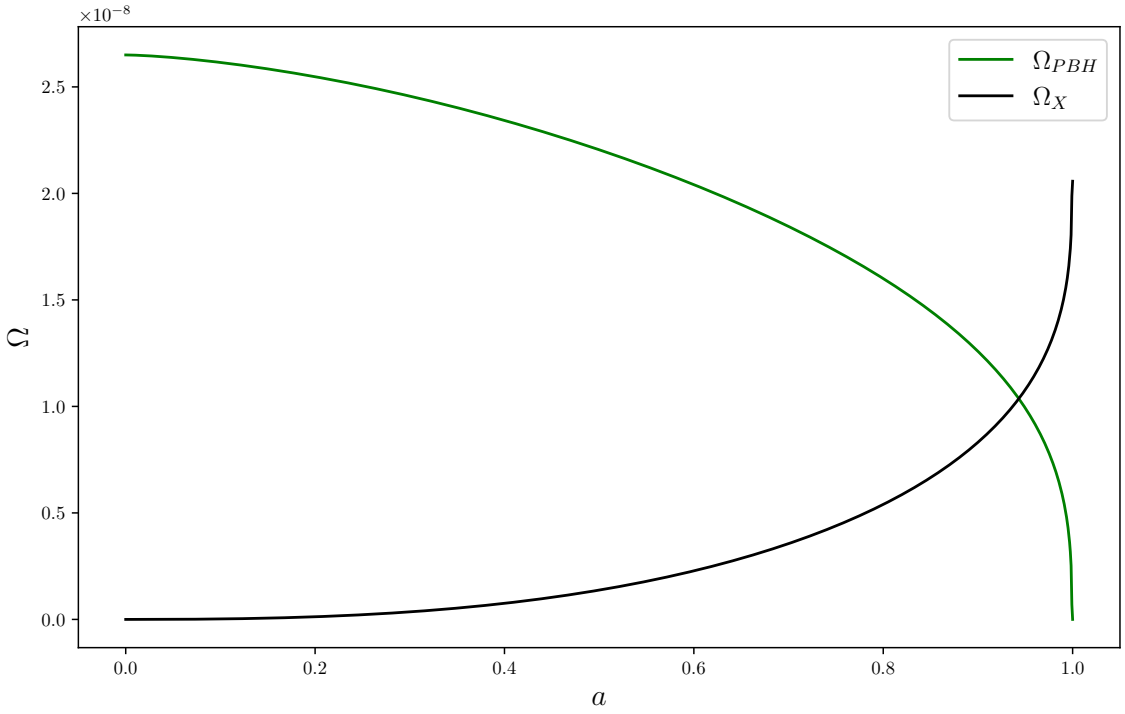

Figure 6.9: $\Omega_{\rm PBH}$ background evolution considering $f_{\rm PBH} = 10^{-7}$ and $M_{\rm in} = 6.46 \times 10^{14}\,\mathrm{g}$.

Annex D

Limited estimation

This appendix contains the confidence contour plots for the PBH model, limited to 10 000 samples, in Figures 6.10 and 6.11.

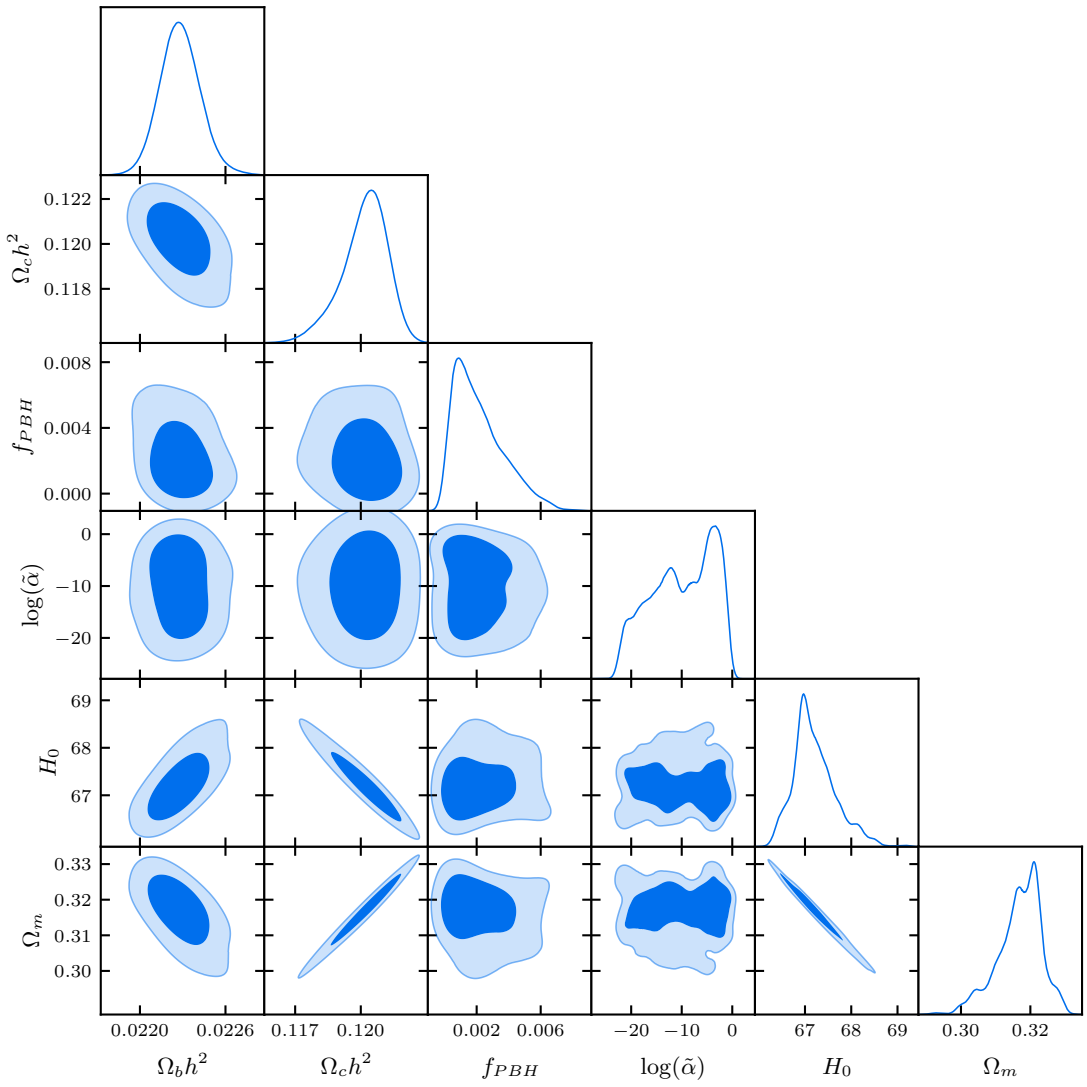

Figure 6.10: The 68 % and 95 % confidence contours for the PBH model, with $\Omega_{\Lambda,0} = 0.6842$ fixed, limited to 10 000 samples.

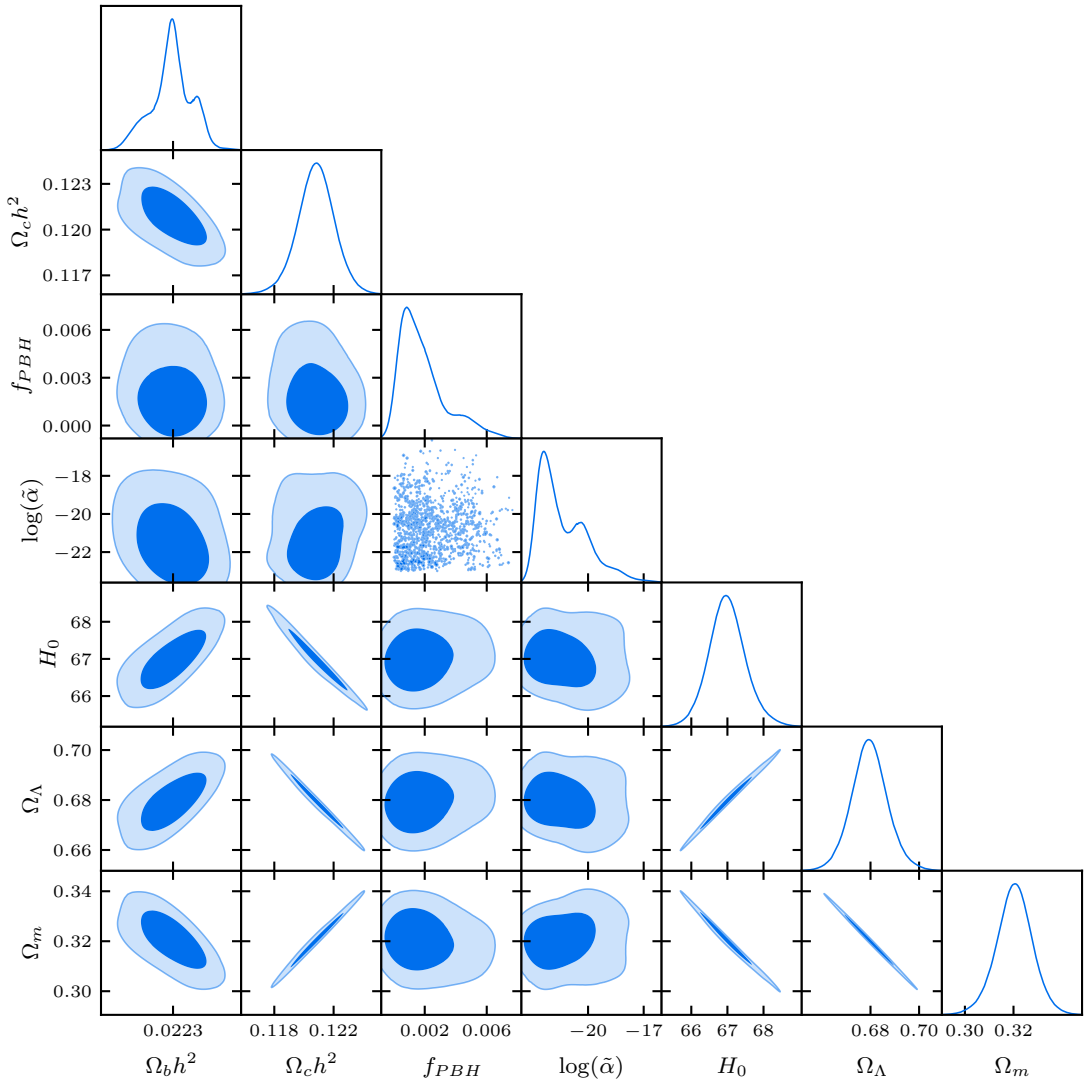

Figure 6.11: The 68 % and 95 % confidence contours for the PBH model, limited to 10 000 samples.